Hindawi
Mathematical Problems in Engineering
Volume 2022, Article ID 4474884, 21 pages
https://doi.org/10.1155/2022/4474884

Research Article

Tube-MPC Control via Notch Filter for Flexible Air-Breathing Hypersonic Vehicle with Actuator Fault

Xiaohe Yang,[1] Weijie Lv,[1] Hanpeng Mi,[1] Chaofang Hu ,[1] and Yongtai Hu[2]

[1]*School of Electrical and Information, Tianjin University, Tianjin 300072, China*
[2]*Aviation Key Laboratory of Science and Technology on Aircraft Control, Xi'an 710065, China*

Correspondence should be addressed to Chaofang Hu; cfhu@tju.edu.cn

Received 3 August 2021; Revised 22 April 2022; Accepted 6 May 2022; Published 30 July 2022

Academic Editor: Hongguang Pan

In this paper, the tube model predictive control (Tube-MPC) via notch filter is proposed for flexible air-breathing hypersonic vehicle with actuator fault. Firstly, considering the low-order flexible modes, the polytopic linear parameter varying (LPV) model of flexible air-breathing hypersonic vehicle is established using Jacobian linearization and tensor product. Actuator fault and parameter uncertainty are transformed into a lumped disturbance term. The baseline Tube-MPC trajectory tracking controller is developed by designing robust auxiliary feedback control law and nominal control law. In order to weaken the effect of flexibility, a notch filter is introduced to eliminate the frequency response peak of flexible modes. And the effect of notch filter on control performance and stability is analysed. Secondly, an alternative controller design strategy is proposed to ensure stability of the closed-loop system. The filter and the original nonlinear model are combined together such that the new polytopic LPV model is codesigned. On the basis, the adjustable Tube-MPC controller is developed to improve the control performance and ensure the stability of the system. Finally, the effectiveness of the two controllers is verified by simulations.

1. Introduction

Air-breathing hypersonic vehicle has the advantages of high-speed and low-launch cost in space transportation and potential of fast global strike in military application [1]. Compared with the traditional aircraft, air-breathing hypersonic vehicle has more significant characteristics such as the interaction of aerodynamic-heating-flexible-propulsion, strong time-varying parameters, and modelling uncertainty. Hence the flexible control system faces new challenges [2].

Since the 1980s, many researchers have devoted to modelling flexible air-breathing hypersonic vehicle. There are two categories of approaches: analytical method based on physical principles and computational fluid dynamics (CFD) method. In the former, the longitudinal nonlinear dynamics model derived by Bolender and DOman [3] is widely applied. This model represents complex interaction among aerodynamics, structural dynamics and propulsion system, and has flexible deformation and vibration. In addition, Waszak et al. [4] establish the fuselage/structure coupling model of hypersonic vehicle using the average axis method and decouple the rigid body from the flexible motion equation. Sudalagunta et al. [5] take six independent displacements of the rigid section to model the flexible deformation. In the latter, the purpose of CFD modelling is to analyse aerodynamics by fluid dynamics and calculate aerodynamic coefficients by data fitting. Lisa [6], David [7], and Parker [8] establish flexible hypersonic vehicle models by means of CFD. Regardless of analytical modelling or CFD modelling, the flexible air-breathing hypersonic vehicle model is strongly nonlinear and coupled, which is very unfavourable to control system.

Many control methods have been applied to the control of hypersonic vehicle, such as linear quadratic regulator

(LQR) [9], feedback linearization control [10], backstepping control [11], sliding mode control [12], intelligent control [13], robust control [14], and adaptive control [15]. For hypersonic vehicle with high nonlinearity and large flight envelope, linear parameter varying (LPV) control has the advantage of simple design and attracted more attentions. When hypersonic vehicle is flying at high speed and large maneuver, flexibility cannot be ignored. Commonly, flexibility includes two modes: known flexibility and unknown flexibility. In the first case, the flexible modes are taken as known states for controller design. Huang et al. [16] build polytopic LPV model for hypersonic vehicle with known flexibility, and design gain-scheduling switch controller. Zhang et al. [17] investigate a novel switching LPV framework based on mode independent/dependent persistent dwell time (PDT/MPDT) switching signals to deal with the case of coexistence of slow maneuver and frequent rapid maneuver. Wu et al. [18] build the LPV model of flexible hypersonic vehicle by utilizing the curve fit and least-squares method and design the nonfragile output tracking controller. When flexibility is unknown, either the observer is designed to estimate and compensate flexibility, or the robustness of closed-loop system is utilized to suppress flexibility. Xu et al. [19] model the coupling among flexibility, rigid body, and the accessional angle of attack caused by wind as unknown disturbance, and design neural network and disturbance observer to deal with the lumped coupling. Sun et al. [20] develop a robust backstepping cruise tracking control scheme with closed-loop finite-time convergence for flexible hypersonic vehicle, where a fixed-time sliding-mode disturbance observer is designed for flexibility, uncertainties, and external disturbances.

In addition, actuator fault possibly occurs [21] due to high-speed and large-maneuver flight. Thereby, online observation and compensation or improvement of controller's robustness are common strategies to handle actuator fault. The former belongs to active fault-tolerant control (FCT) method and the latter is passive approach. For example, Zhao et al. [22] develop FTC strategy based on direct Lyapunov method and the bilinear matrix inequalities technique for flexible hypersonic vehicle. An et al. [23] regard the flexible dynamics as equivalent disturbances, and design disturbance observer and sliding-mode tracking controller for flexible hypersonic vehicle ith actuator fault. In order to identify the lumped effect involving flexible modes and actuator fault online, Shao et al. [24] propose neural estimator based on hysteresis quantizer to achieve appointed-time tracking of flexible hypersonic vehicle. In passive FTC research, a weighted LPV Tube-MPC is proposed for hypersonic vehicle with three kinds of actuator fault [25]. The passive fault-tolerant tracking problem is investigated for the bounded external disturbance and sensor fault [26].

Model predictive control (MPC) is popular due to its good ability of handling constraint, and LPV model is generally combined for controller design [27, 28]. This control method is often applied to control complex nonlinear systems. For example, based on the LPV model of unmanned airship, a gain-scheduling MPC controller was designed for lateral control [29]. A systematic design procedure for approximate explicit MPC is presented for constrained nonlinear systems described in LPV form [30]. One-step ahead robust MPC for LPV model with bounded disturbance is developed [31]. Similarly, MPC and LPV are also applicable to hypersonic vehicle, which can effectively deal with the nonlinearity and uncertainty of hypersonic vehicle model. For example, a novel parameter-dependent robust MPC (PD-RMPC) algorithm with explicit time-delay compensation is presented for hypersonic vehicle.

Inspired by the previous work, a Tube-MPC control strategy with north filter is proposed for flexible air-breathing hypersonic vehicle with loss of actuator effectiveness fault in the presence of parameter uncertainty. The weak coupling between flexibility and rigid body is ignored, by which the continuous LPV model of vehicle is established by Jacobian linearization. And the corresponding polytopic formulation is built by tensor product. Parameter uncertainty or actuator fault are uniformly transformed into an additional disturbance term. On the basis, baseline Tube-MPC controller is designed, where robust auxiliary feedback control law and nominal control law are calculated, respectively. The nominal control law provides a reasonable reference trajectory for the actual system. The robust auxiliary feedback control law steers the actual trajectory into the mRPI set and makes it approximate the nominal trajectory. In order to reduce the flexible effect, a notch filter is introduced into the short-period mode. Moreover, the effect of notch filter on the control system is analysed. Alternatively, in order to ensure the stability of the closed-loop system, the transfer function model of filter is transformed into state-space equation. The states of filter and filtered pitch rate are both combined with the original nonlinear model. Considering the weak coupling between flexibility and rigid body, the new polytopic LPV model with notch filter is codesigned. To improve control performance and reduce conservatism, an adjustable Tube-MPC controller is developed. The simulation results show that the two types of Tube-MPC design method with notch can both effectively get rid of the elastic effect and provide good tracking performance.

The rest of this paper is organized as follows. Firstly, the nonlinear longitudinal model of hypersonic vehicle is presented. Secondly, the control-oriented polytopic LPV model is established and the baseline Tube-MPC controller design via notch filter is proposed. Then, the adjustable Tube-MPC controller based on the codesigned polytopic LPV model is presented. The effectiveness of these two strategies is verified by simulations. Finally, conclusion is drawn.

2. Flexible Hypersonic Vehicle Model

The flexible hypersonic vehicle is regarded as a pair of cantilever beams and assumed to follow Hook's law. The longitudinal dynamic equations (Coupling model, CM) are introduced [8], which consists of rigid body motion equations and flexible vibrations.

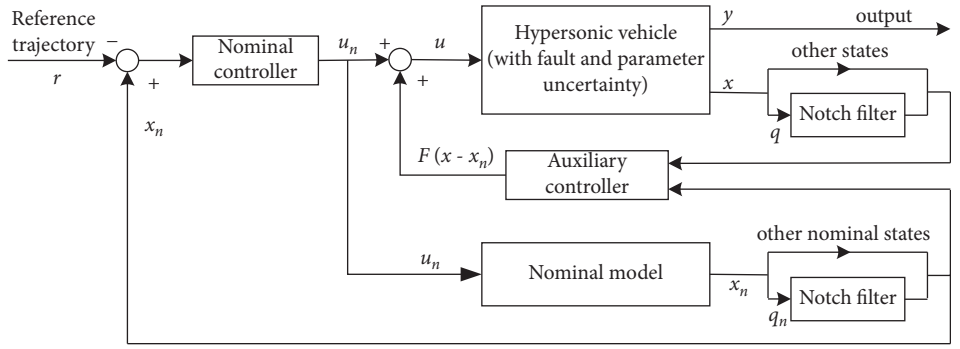

Figure 1: Baseline Tube-MPC scheme.

$$\begin{aligned}
\dot{h} &= V\sin(\theta-\alpha),\\
\dot{V} &= \frac{1}{m}(T\cos\alpha - D) - g\sin(\theta-\alpha),\\
\dot{\alpha} &= \frac{1}{mV}(-T\sin\alpha - L) + q + \frac{g}{V}\cos(\theta-\alpha),\\
\dot{\theta} &= q,\\
\dot{q} &= \frac{1}{I_{yy}}(M + \widetilde{\psi}_1\ddot{\eta}_1 + \widetilde{\psi}_2\ddot{\eta}_2),\\
\ddot{\eta}_1 &= \frac{1}{k_1}\left(-2\zeta_1\omega_1\dot{\eta}_1 - \omega_1^2\eta_1 + N_1 - \widetilde{\psi}_1\frac{M}{I_{yy}} - \frac{\widetilde{\psi}_1\widetilde{\psi}_2\ddot{\eta}_2}{I_{yy}}\right),\\
\ddot{\eta}_2 &= \frac{1}{k_2}\left(-2\zeta_2\omega_2\dot{\eta}_2 - \omega_2^2\eta_2 + N_2 - \widetilde{\psi}_2\frac{M}{I_{yy}} - \frac{\widetilde{\psi}_2\widetilde{\psi}_1\ddot{\eta}_1}{I_{yy}}\right),
\end{aligned} \tag{1}$$

where h, V, α, θ, q are altitude, velocity, attack angle, pitch angle, and pitch rate, respectively; m, I_{yy}, g are quality, moment of inertia, and gravitational acceleration, respectively. η_i represent the generalized flexible coordinates of the ith flexible mode; $\zeta_i, \omega_i, \widetilde{\psi}_i$ are natural frequencies, damping ratios and inertial coupling parameter of the ith flexible mode, respectively. $k_i = 1 + \widetilde{\psi}_i^2/I_{yy}$. In addition, L, D, T, and M denote lift, drag, thrust, and pitching moment, respectively, and N_i denotes the generalized force of the ith flexible mode. They are expressed by the following curve-fitting approximation:

$$\begin{aligned}
L &= \overline{q}SC_L(\alpha,\delta_e),\\
D &= \overline{q}SC_D(\alpha,\delta_e),\\
T &= C_T^{\alpha^3}\alpha^3 + C_T^{\alpha^2}\alpha^2 + C_T^{\alpha}\alpha + C_T^0\\
M &= z_T + \overline{q}S\overline{c}\left(C_{M,\alpha}(\alpha) + C_{M,\delta_e}(\delta_e)\right),\\
N_1 &= N_1^{\alpha^2}\alpha^2 + N_1^{\alpha}\alpha + N_1^0,\\
N_2 &= N_2^{\alpha^2}\alpha^2 + N_2^{\alpha}\alpha + N_2^{\delta_e}\delta_e + N_2^0,
\end{aligned} \tag{2}$$

where δ_e is the elevator deflection. $\overline{q}$ is the dynamic pressure. $S, z_T, \overline{c}$ represent reference area of vehicle, thrust to moment coupling coefficient, and mean aerodynamic chord, respectively. $\overline{q}$ and coefficients of the nonlinear model are calculated as

$$\begin{aligned}
\overline{q} &= \frac{1}{2}\rho V^2,\\
\rho &= \rho_0 e^{-h-h_s/h_0},\\
C_L &= C_L^{\alpha}\alpha + C_L^{\delta_e}\delta_e + C_L^0,\\
C_D &= C_D^{\alpha^2}\alpha^2 + C_D^{\alpha}\alpha + C_D^{\delta_e^2}\delta_e^2 + C_D^{\delta_e}\delta_e + C_D^0,\\
C_{M,\alpha} &= C_{M,\alpha}^{\alpha^2}\alpha^2 + C_{M,\alpha}^{\alpha}\alpha + C_{M,\alpha}^0,\\
C_{M,\delta_e} &= c_e\delta_e,\\
C_T^{\alpha^3} &= \beta_1(h,\overline{q})\Phi + \beta_2(h,\overline{q}),\\
C_T^{\alpha^2} &= \beta_3(h,\overline{q})\Phi + \beta_4(h,\overline{q}),\\
C_T^{\alpha} &= \beta_5(h,\overline{q})\Phi + \beta_6(h,\overline{q}),\\
C_T^0 &= \beta_7(h,\overline{q})\Phi + \beta_8(h,\overline{q}),
\end{aligned} \tag{3}$$

where ρ is the air density, $\rho_0, h_0, 1/h_s$ are the air density at nominal altitude, nominal altitude for air density approximation, and air density decay rate, respectively. Φ is the fuel-to-air ratio; c_e is the elevator coefficient; $\beta_i(h,\overline{q}), i = 1, 2, \ldots, 8$ are thrust parameters.

3. Tube-MPC via Notch Filter

For longitudinal trajectory tracking of flexible air-breathing hypersonic vehicle in presence of uncertain parameter and actuator fault, the baseline Tube-MPC controller is designed [32]. Meanwhile, a notch filter is introduced to suppress flexibility. The schematic of the closed-loop control system is shown in Figure 1.

3.1. Control-Oriented Polytopic LPV Modelling. To linearize nonlinear vehicle model, the weak coupling between the rigid body and the flexible modes is ignored (called Decoupling Model, DM). The following longitudinal motion equations are adopted [16]:

$$\begin{aligned}
\dot{h} &= V\sin(\theta-\alpha),\\
\dot{V} &= \frac{1}{m}(T\cos\alpha - D) - g\sin(\theta-\alpha),\\
\dot{\alpha} &= \frac{1}{mV}(-T\sin\alpha - L) + q + \frac{g}{V}\cos(\theta-\alpha),\\
\dot{\theta} &= q,\\
\dot{q} &= \frac{M}{I_{yy}},\\
\ddot{\eta}_1 &= -2\zeta_1\omega_1\dot{\eta}_1 - \omega_1^2\eta_1 + N_1,\\
\ddot{\eta}_2 &= -2\zeta_2\omega_2\dot{\eta}_2 - \omega_2^2\eta_2 + N_2.
\end{aligned} \tag{4}$$

In this paper, the polytopic LPV model of DM is built by Jacobian linearization and tensor product.

Firstly, within the flight envelope, altitude and velocity are selected as scheduling variables, denoted as $p(t) = [h, V]^T \in \Gamma$. Then, Jacobian linearization is performed at each equilibrium point. Define $x_s = [h, V, \alpha, \theta, q, \eta_1, \dot{\eta}_1, \eta_2, \dot{\eta}_2]$ and $u_s = [\Phi, \delta_e]$. To compute the equilibrium points of flexible vehicle, let $\dot{x}_s = l_i(x_s, u_s) = 0, i = 1, 2, \ldots, 9$. According to the selected height h_r and velocity V_r, the states and control inputs at the equilibrium point are described as

$$\begin{aligned}
x_r &= \left[h_r, V_r, \alpha_r(h,V), \theta_r(h,V), q_r(h,V), \eta_{1r}(h,V), \dot{\eta}_{1r}(h,V), \eta_{2r}(h,V), \dot{\eta}_{2r}(h,V)\right]^T,\\
u_r &= \left[\Phi_r(h,V), \delta_{er}(h,V)\right]^T.
\end{aligned} \tag{5}$$

Define the neighbourhood of equilibrium point as $l(x_s, u_s)$. The first-order Taylor series expansion is performed as

$$\begin{aligned}
l(x_s,u_s) \approx\ & l(x_r,u_r) + \frac{\partial l(x_s,u_s)}{\partial x_s}\Big|_{x_s=x_r}(x_s - x_r)\\
&+ \frac{\partial l(x_s,u_s)}{\partial u_s}\Big|_{u_s=u_r}(u_s - u_r).
\end{aligned} \tag{6}$$

Define new state variables and control inputs as

$$\begin{aligned}
x &= x_s - x_r = [\Delta h, \Delta V, \Delta\alpha, \Delta\theta, \Delta q, \Delta\eta_1, \Delta\dot{\eta}_1, \Delta\eta_2, \Delta\dot{\eta}_2],\ u = u_s\\
&\quad - u_r = [\Delta\Phi, \Delta\delta_e].
\end{aligned} \tag{7}$$

Then,

$$\dot{x} = \dot{x}_s - \dot{x}_r = l(x_s,u_s) - l(x_r,u_r) = \frac{\partial l(x_s,u_s)}{\partial x_s}\Big|_{x_s=x_r} x + \frac{\partial l(x_s,u_s)}{\partial u_s}\Big|_{u_s=u_r} u. \tag{8}$$

Further, model (4) is rewritten as

$$\dot{x}(t) = Ax(t) + Bu(t), \tag{9}$$

where $A = \partial l(x_s,u_s)/\partial x_s, B = \partial l(x_s,u_s)/\partial u_s$. Obviously, equation (6) is a linear time-varying (LTI) system.

Within the flight envelope, multiple equilibrium points are selected for Jacobian linearization. The corresponding LTI systems are fitted into the following continuous LPV model:

$$\dot{x}(t) = A(p(t))x(t) + B(p(t))u(t). \tag{10}$$

where $A(p(t))$ and $B(p(t))$ are matrices with scheduling variables.

The continuous LPV model (7) is transformed into a polytopic LPV system by tensor product [33].

Assuming that m singular values are determined in height and n singular values in velocity, a polytopic LPV system with $R_l = m \times n$ vertices is obtained. A time-varying matrix is defined as $S(p(t)) = [A(p(t)), B(p(t))]$, expressed by a convex combination of vertex systems

$$S(p(t)) \underset{\xi}{\approx} \sum_{i=1}^{R_l} \tau_i(p(t)) S_i, \tag{11}$$

where $S_i, i = 1, \ldots, R_l$ represents each vertex system, $\tau_i(p(t))$ is the weight coefficient of each vertex system being dependent on scheduling variables, and $\sum_{i=1}^{R_l} \tau_i = 1$. ξ is the modelling error between the original nonlinear model and the polytopic LPV model.

The above polytopic LPV model is discretized, and there is

$$x(k+1) = A(p(k))x(k) + B(p(k))u(k), \tag{12}$$

where $[A(p(k)), B(p(k))] \in \Omega = Co\{[A_1, B_1], \ldots [A_{R_l}, B_{R_l}]\}$. $[A_i, B_i], i = 1, \ldots, R_l$ are the polytopic vertices, Ω is the convex set, and Co is the convex hull. $[A(p(k)), B(p(k))] = \sum_{i=1}^{R_l} \tau_i(k)[A_i, B_i]$, and $\sum_{i=1}^{R_l} \tau_i(k) = 1$, $0 \le \tau_i(k) \le 1$.

The Bode diagram of the DM model and the polytopic LPV model are drawn at any point in the flight envelope. As shown in the figure, the solid red line represents the DM system, and the dotted blue line for the polytopic LPV system. It can be seen that the two lines overlap very well. In other words, the established LPV model has high accuracy.

Due to aeroelastic deformation during flight, moment of inertia, reference area, and some aerodynamic parameters of hypersonic vehicle will change. Considering the uncertain parameters and linearization modelling error, the following model is obtained:

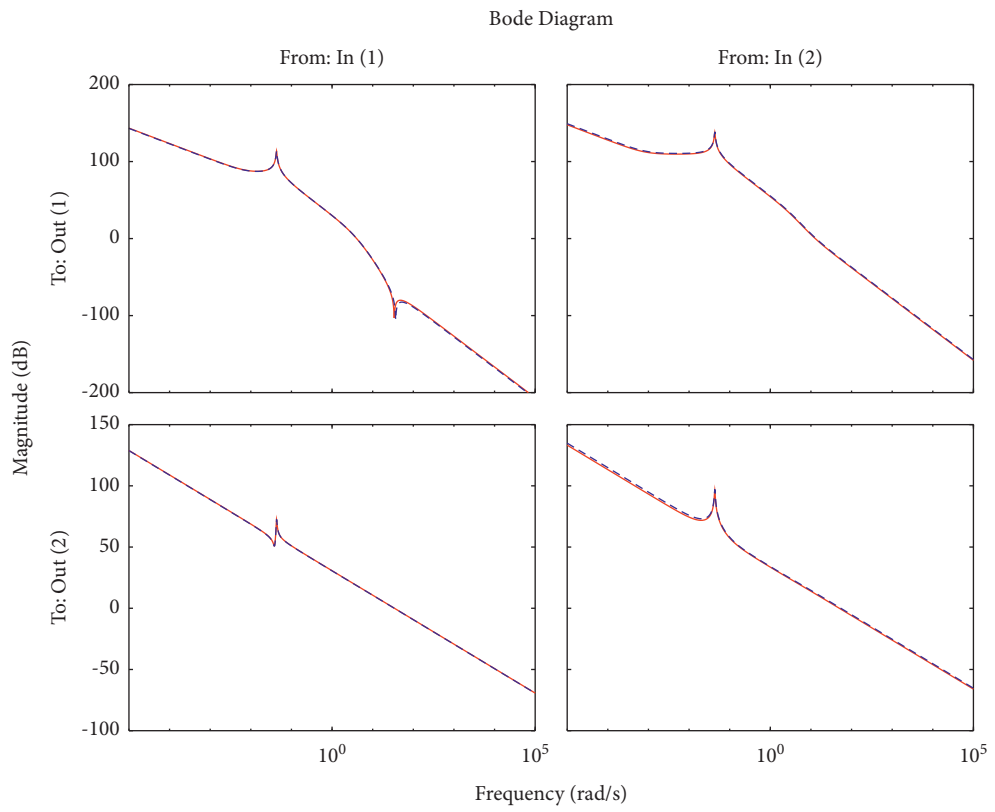

(a)

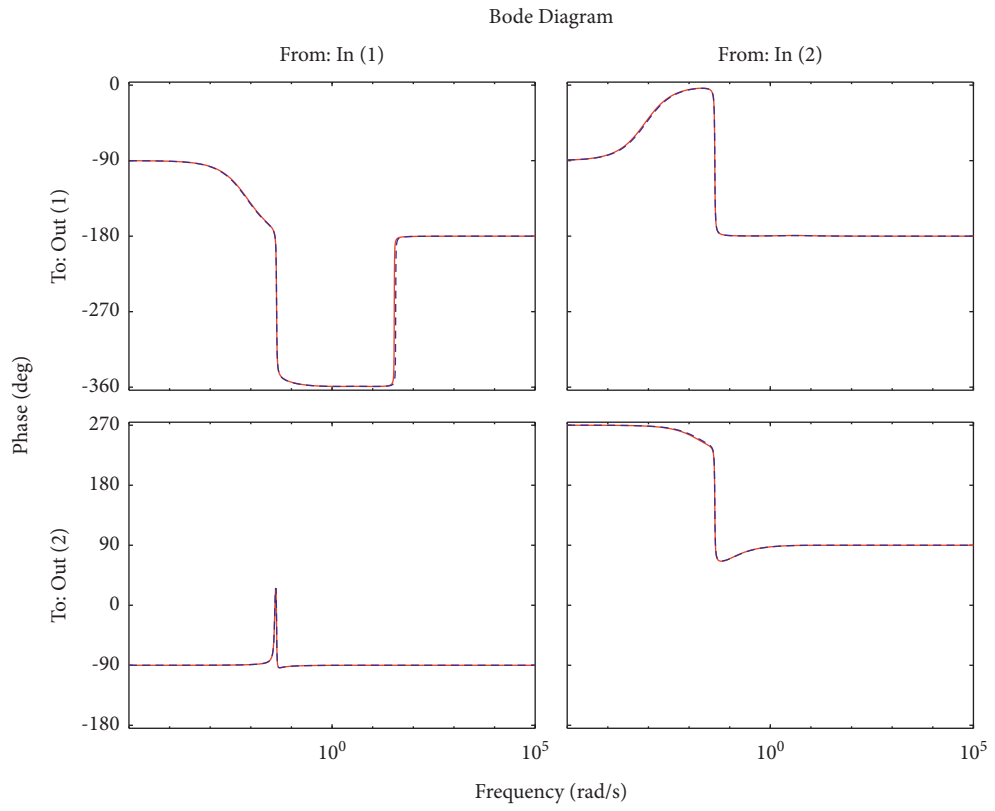

(b)

Figure 2: Bode diagram comparison of polytopic LPV and DM. (a) Amplitude frequency characteristic. (b) Phase frequency characteristic.

$$x(k+1) = A(p(k))x(k) + B(p(k))u(k) + f, \tag{13}$$

f is a summarized term resulting from parameter uncertainty and modelling error. It is assumed that f is bounded, i.e., $f \in W_1 = \{f \in R^9 | -|f|_{\min} \le f \le |f|_{\max}\}$.

In some cases, actuator faults may occur during vehicle flying. Loss of effectiveness fault is addressed in this paper and its corresponding faulty model is written as

$$x(k+1) = A(p(k))x(k) + B(p(k))u_f(k) + f, \tag{14}$$

where u_f is the control inputs with loss of effectiveness fault occurring on elevator.

$$u_f = \begin{bmatrix} 1 & 0 \\ 0 & \rho_f \end{bmatrix} \begin{bmatrix} \Phi \\ \delta_e \end{bmatrix} = \mathrm{P}u. \tag{15}$$

Then,

$$x(k+1) = A(p(k))x(k) + B(p(k))u(k) + f + w, \tag{16}$$

where $w = B(p(k))(\mathrm{P} - I)u$, and w is bounded, that is,

$$\begin{aligned} w \in W_2 = \{w \in R^9 | &-|B(p(k))(\mathrm{P} - I)u|_{\min} \\ &\le w \le |B(p(k))(\mathrm{P} - I)u|_{\max}\}. \end{aligned} \tag{17}$$

In summary, uncertain parameters, modelling error, and actuator failure of flexible hypersonic vehicle can be lumped into a bounded term Δ. Thereby, model (11) is rewritten as

$$x(k+1) = A(p(k))x(k) + B(p(k))u(k) + \Delta, \tag{18}$$

where $\Delta = f + W$ and Δ is bounded, that is,

$$\Delta \in W = \{\Delta \in R^9 | -|\Delta|_{\min} \le \Delta \le |\Delta|_{\max}\}. \tag{19}$$

Remark 1. In polytopic LPV modelling, the uncertain term f caused by uncertain parameters, the disturbance term w caused by actuator faults, and the lumped term Δ are all assumed to be bounded. In controller design, the worst conditions will be considered to obtain the maximum robustness, f, w, Δ are taken as maximum or minimum.

3.2. Baseline Tube-MPC Controller Design. For model (14), the nominal system is defined as

$$x_n(k+1) = A(p(k))x_n(k) + B(p(k))u_n(k), \tag{20}$$

where x_n are nominal states and u_n are nominal control inputs.

The Tube-MPC control law is designed as

$$u(k) = F(x(k) - x_n(k)) + Kx_n(k), \tag{21}$$

where K is the nominal control gain used to generate a nominal trajectory and F is the auxiliary robust feedback gain to reject the lumped term. The control law (16) forces the trajectory of the actual system into mRPI set and the actual trajectory will get close to the nominal.

Firstly, the robust feedback control gain F is designed. The control errors between the actual system and the nominal system are defined as $e(k) = x(k) - x_n(k)$. Then, by subtracting (15) from (14), the following error equation can be obtained:

$$e(k+1) = (A(p(k)) + B(p(k)F)e(k) + \Delta). \tag{22}$$

It can be known that $e(k)$ is bounded when $(A(p(k))) + B(p(k)F)$ satisfies the conditions of Hurwitz matrix.

The system without parameter uncertainty is defined as

$$e\prime(k+1) = (A(p(k))) + B(p(k)F)e\prime(k). \tag{23}$$

The auxiliary robust feedback control gain F is solved by the following lemma.

Lemma 1. *(see [34]) For polytopic LPV systems (18), if there are matrix $M_F, N_F > 0$, so that the following LMI holds:*

$$\begin{bmatrix} N_F & (A(p(k))N_F + B(p(k))M_F)^T \\ (A(p(k))N_F + B(p(k))M_F) & N_F \end{bmatrix} > 0, A(p(k)), B(p(k)) \in \Omega. \tag{24}$$

Then the auxiliary robust feedback control gain $F = M_F N_F^{-1}$ can ensure the stability of system (18).

To compute mRPI set, the following definition is given.

Definition 1. (see [35]) The set $Z \in R^9$ is the mRPI set of the polytopic LPV system (14) if and only if there is $e(k+1) \in Z$ for all error states $e(k) \in Z$, $[A(p(k)), B(p(k))] \in \Omega$ and $\Delta \in W$.

From Definition 1, we know that $e(k)$ is always located in the mRPI set. Therefore, $x = (x_n \oplus Z)$ holds, where $\oplus$ is Minkowski set addition. Due to W being symmetric around the origin, the mRPI set Z has the same symmetric characteristic around the origin. Consequently, the mRPI set of model (14) is defined as

$$Z = \{e(k) \in R^9 | -z \le e(k) \le z, z > 0\}, \tag{25}$$

where z is the upper bound.

For $\forall \Delta \in W$, Z satisfies the following equation:

$$(A(p(k)) + B(p(k))F)Z \oplus W \subseteq Z. \tag{26}$$

Thereby, the constraint (21) can be converted to

$$\begin{aligned} I_i^T((A(p(k)) + B(p(k))F)e(k) + \Delta) \le I_i^T z, \\ \forall e(k) \in Z, \forall \Delta \in W, i = 1, 2, \ldots, 9, \end{aligned} \tag{27}$$

where $I \in R^{9\times 9}$ is the identity matrix.

In order to enhance robustness, it is expected that the invariant set becomes as small as possible. Define $\gamma = \sum_{i=1}^{9} z_i$, where z_i is the maximum value of each column. By

minimizing γ, the boundary of Z is solved, and the best robustness is achieved. Farkas lemma is introduced to solve mRPI set Z.

Lemma 2 (see [36]). *For $d \in R^n, n \in R, A \in R^{d\times n}, b \in R^d$, if there is $\hat{c}$ satisfying $A\hat{c} < b$, then the following two statements are equivalent.*

(1) $d^T c \le n$, such that $Ac < b$,

(2) $\exists \rho \in R^m$ such that $\rho \ge 0, A^T\rho = d, b^T\rho \le n$.

The optimization problem for the mRPI set is formulated as follows:

$$\begin{aligned}
&\min\ \gamma,\\
&s.t.\ \rho_W^i \ge 0, \rho_W^i + EI_i \ge 0, \rho_{e(x)}^i \ge 0,\\
&\rho_{e(k)}^i + \left(A\left(p(k)Z_d\right) + B(p(k))FZ_d\right)^T \ge 0, \qquad \sum_{i=1}^{9} I_i^T Z_d I_i \ge 0. \qquad (28)\\
&I_i^T Z_d I - W_1^T\left(2\rho_W^i + EI\right) - I^T\left(2\rho_{e(k)}^i + \left(A\left(p(k)Z_d\right) + B(p(k))FZ_d\right)^T I_i\right) \ge 0,\\
&\gamma - \sum
\end{aligned}$$

where $\rho_{W_1}^i \in R^{9_{W_1}}, \rho_{e(k)}^i \in R^9, Z_d = diag(Z)$, I_i is the n-dimensional unit vector, and $E \in R^{9\times 9}$ is the interference distribution matrix. Then, $z = Z_d I_i$, and Z can be obtained by (20).

Consider the control input constraints of flexible hypersonic vehicle

$$u(k) \in U \coloneqq = \left\{u \in R^2 \| u(k) \| \le u_{\max}\right\}, \qquad (29)$$

where $u_{\max}$ represents the maximum of control inputs.

Based on the auxiliary robust feedback control gain F and the mRPI set Z, the control inputs of the nominal system should satisfy

$$u_n(k) \in \chi \coloneqq = \left\{u_n \in R^2 | U\Theta FZ\right\}, \qquad (30)$$

where Θ is the Pontryagin set difference, and there is $U\Theta FZ \ne \varnothing$.

The nominal control law at the vertex of each convex hull is designed to provide an appropriate nominal trajectory. For system (15), the following infinite time-domain quadratic programming performance index is given:

$$\min_K \max_{[A(p(k)),B(p(k))]\in\Omega} J_\infty(k) = \sum_{i=0}^{\infty}\left[\left\|x_n(k+i|k)\right\|_\psi^2 + \left\|u_n(k+i|k)\right\|_\sigma^2\right], \qquad (31)$$

where $\psi > 0, \sigma > 0$.

If there are matrix $Y \in R^{2\times 9}$, symmetric matrix $Q \in R^{9\times 9}$, and a positive scalar γ_n, such that all polytopic vertices $[A_i, B_i], i = 1, \ldots, R_l$ satisfying the following optimization problem, the nominal control law $u_n(k) = Kx_n(k) = YQ^{-1}x_n(k)$ can stabilize system.

$$\min_{\gamma_n, Y, G, Q} \gamma_n, \qquad (32)$$

$$s.t\begin{bmatrix} 1 & x_n(k)^T \\ x_n(k) & Q \end{bmatrix} \ge 0, \qquad (33)$$

$$\begin{bmatrix} Q & Q^T A_i^T + Y^T B_i^T & Q^T \psi^{1/2T} & Y^T \sigma^{1/2T} \\ {}_A^i Q + {}_B^i Y & Q & 0 & 0 \\ \psi^{1/2} Q & 0 & \gamma_n I & 0 \\ \sigma^{1/2} Y & 0 & 0 & \gamma_n I \end{bmatrix} > 0, \quad i \in \{1, 2, \ldots, R_l\}, \qquad (34)$$

$$\begin{bmatrix} X & Y \\ Y^T & Q \end{bmatrix} \ge 0, X = \begin{bmatrix} u_{n1} & 0 \\ 0 & u_{n2} \end{bmatrix}, u_{nj} \le u_{nj,\max}^2, j = 1, 2, \qquad (35)$$

where $u_{nj,\max}^2$ is the maximum of the jth nominal input.

The quadratic programming criterion "min-max" (26) is converted to minimization of the upper bound γ_n, that is, a new minimum optimization problem (32) is formulated [37]. LMI constraint (33) guarantees that the nominal states stay in the invariant set with respect to the nominal control law $u_n(k)$, i.e., $x_n(k|k) = x_n(k) \in \Omega$, and $\Omega = \left\{x_n \in R^9 | x_n^T Q x_n \le 1\right\}$. Equation (34) indicates that the Lyapunov function of the nominal system (15) is decreasing [37]. Equation (35) is derived from the input constraint $|u_{nj}| \le u_{nj,\max}$.

In conclusion, the nominal control law $u_n(k) = Kx_n(k) = YG^{-1}x_n(k)$ can guarantee the stability of the nominal system (15).

The real control law is written as

$$u_{total} = F\left(x - x_n\right) + Kx_n + u_r, \qquad (36)$$

where u_r is the control input at the equilibrium point.

3.3. Notch Filter Design. The Tube-MPC controller designed above can guarantee the stability of the rigid body states and flexible states of hypersonic vehicle with actuator faults. In order to further handle flexibility and reduce the coupling originating from flexible modes, a notch filter is introduced in this paper. The notch filter can reduce the flexible vibration as much as possible by eliminating the peak of flexible mode frequency response [38, 39].

The frequency response of an ideal notch filter is described as

$$H\left(e^{j\omega t}\right) = \begin{cases} 0, \omega = \omega_f \\ 1, \omega \neq \omega_f \end{cases}, \tag{37}$$

where ω_f is the notch frequency.

A notch filter should have the following two characteristics.

(1) The notch is deep enough and has a certain width. All zeros of transfer function of notch filter should be on the unit circle.

(2) Non-notch frequency signals are unaffected. The zero-pole of transfer function of notch filter must match.

The transfer function of notch filter is [38]

$$H(s) = \frac{1/\omega_z^2 s^2 + 2\varepsilon_z/\omega_z s + 1}{1/\omega_p^2 s^2 + 2\varepsilon_p/\omega_p s + 1}, \tag{38}$$

where ω_z, ω_p are frequency and $\varepsilon_z, \varepsilon_p$ are damping ratio.

In equation (33), the numerator transmission function can determine the frequency of the notch centre. The denominator transmission function is used for the physical implementation of notch filter.

From CM (1), it can be seen that the coupling between rigid body states and the flexible modes is mainly reflected in pitch rate q. Therefore, a notch filter is introduced into the feedback of q channel. The open-loop Bode diagram is presented as Figure 3, to analyse the effect of notch filter on flexible hypersonic vehicle.

From the figure, it can be seen that the peak caused by the flexible mode is suppressed after the notch filter is connected into the flexible hypersonic vehicle. The different parameter alternation of notch filter has the similar effect as [40]. In conclusion, the reasonable choice of notch filter will not destroy the stability of the original system.

For the effects of the first-order and second-order flexible modes on hypersonic vehicle, we linearize CM (1) at equilibrium point based on small disturbance linearization, and the open-loop pole distribution diagram is drawn in Figure 4.

From Figure 4, it can be seen that CM (1) has a total of 7 motion modes, including five motion modes of rigid body and two aeroelastic modes. Two flexible modes correspond to two pairs of underdamped conjugate complex roots, whose natural frequencies are almost consistent with the natural frequencies of structural flexibility. Since the two pairs of underdamped conjugate complex roots are close to the imaginary axis, both of the two flexible modes have a great influence on CM (1). Therefore, the notch filter is designed for the first- and second-order flexible modes, respectively. Only single one flexible mode is focused. However, by means of reasonable selection of notch filter parameters, it is possible to reduce the other flexible mode while suppressing the focused one. Take the first-order flexible mode as an example, as shown in Figure 5. The first-order flexible mode is the centre of notch filter and aimed to be cancelled. Meanwhile, the second-order flexible mode is partially decreased at the edge of notch filter.

After the notch filter is introduced, the system stability of flexible hypersonic vehicle can still be guaranteed by control law (31). The reasons are as follows.

First of all, the principle of notch filter is that the non-notch frequency is not affected, so only the first flexible mode is filtered out. As previously analysed, the appropriate parameter selection of notch filter will not destroy the stability of the original system, and will even increase the phase margin of the system.

Secondly, the model parameter uncertainty, including M, I_{yy} and other 10 parameters, is considered while designing Tube-MPC controller. These uncertainties are caused by many factors such as flexibility, fuel consumption, and flight environment change. With the Tube-MPC controller, the actual states of system are limited within the mRPI set and are constantly approximating the nominal trajectory. The filtering of first flexible mode can actually be regarded as the reduction of the model parameter uncertainty. In this paper, the mRPI set is designed on the basis of maximum parameter uncertainty. Therefore, the system states still stay in mRPI set after filtering. At the same time, compared with the system without notch filter, the position of system states with notch filter in the mRPI set is closer to the nominal trajectory, as shown in Figure 6. Therefore, the control law (31) can still ensure the stability of flexible hypersonic vehicle. Moreover, the performance of system with notch filter is better than without notch filter.

4. An Adjustable Controller Design Scheme

In this paper, an alternatively adjustable controller based on the codesigned polytopic LPV model is proposed to ensure the stability of the system. Filter states and output are introduced into the original model to formulate an extended states coupling model (ECM). The new polytopic LPV model is codesigned using the same linearization method for the weak coupling between flexibility and rigid body. To improve the control performance, the adjustable Tube-MPC controller is designed. The schematic of the new control system is shown in Figure 7.

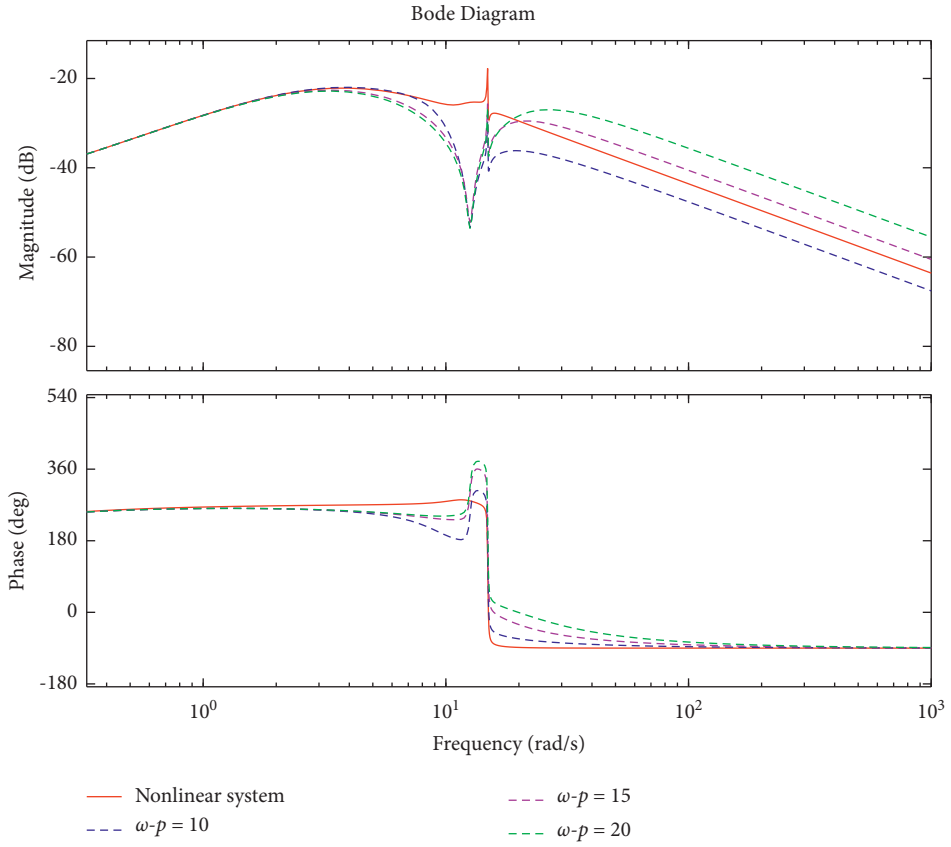

(a)

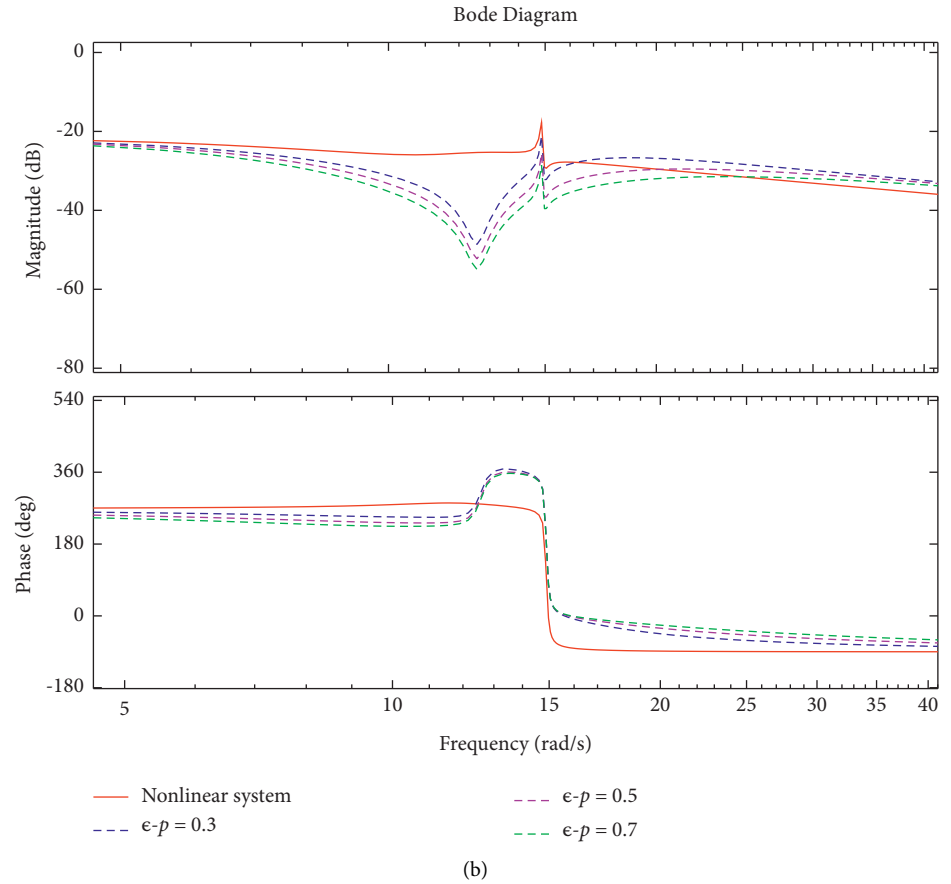

(b)

FIGURE 3: Bode diagram of notch filter's effect on flexible hypersonic vehicle. (a) Effect of ω_p when $\varepsilon_p = 0.5$. (b) Effect of ε_p when.$\omega_p = 15$.

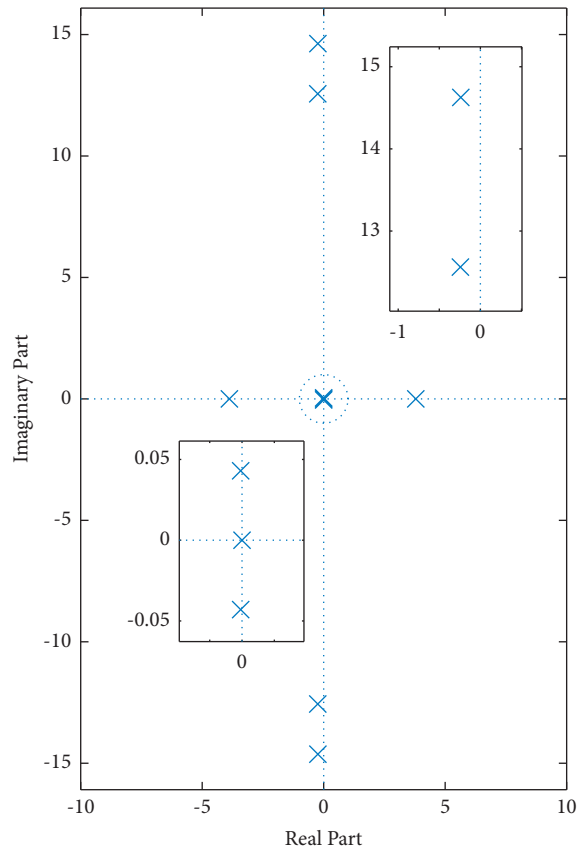

Figure 4: Open-loop pole distribution.

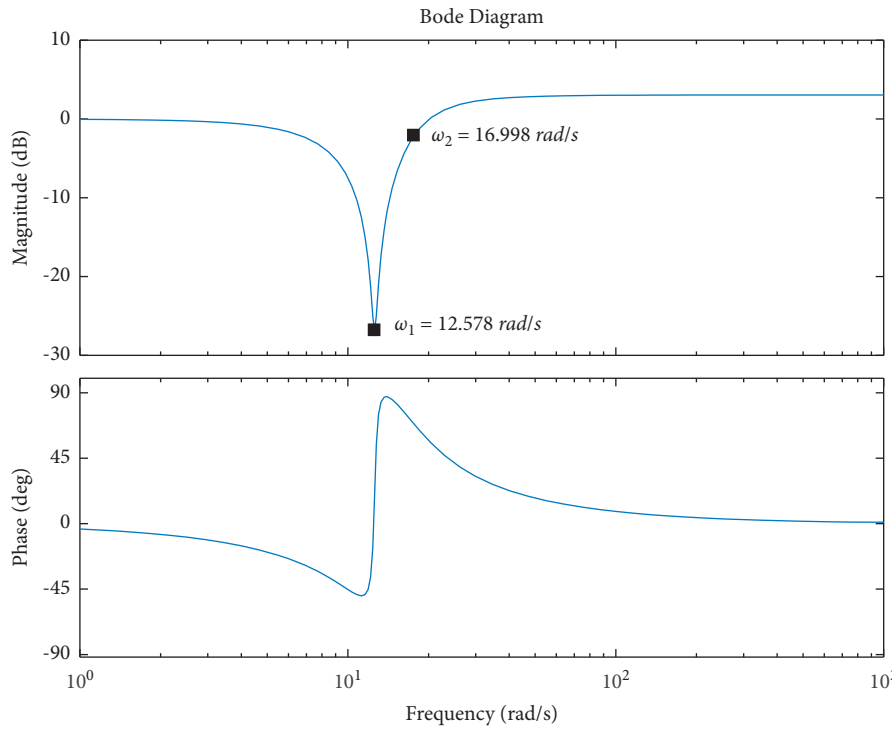

Figure 5: Bode diagram of Notch filter on flexible modes.

4.1. ECM Modelling. Convert the transfer function of notch filter into state space equation, as follows:

$$\begin{bmatrix} \dot{x}_{q1} \\ \dot{x}_{q2} \end{bmatrix} = \begin{bmatrix} a_{q1} & a_{q2} \\ a_{q3} & a_{q4} \end{bmatrix} \begin{bmatrix} x_{q1} \\ x_{q2} \end{bmatrix} + \begin{bmatrix} b_{q1} \\ b_{q2} \end{bmatrix} q,$$
$$q' = \begin{bmatrix} c_{q1} & c_{q2} \end{bmatrix} \begin{bmatrix} x_{q1} \\ x_{q2} \end{bmatrix} + d_q q, \tag{39}$$

where x_{q1}, x_{q2} are states of notch filter, respectively; q' is output of filter, that is, the filtered pitch rate; $a_{q1,2,3,4}, b_{q1,2}, c_{q1,2}, d_q$ are the parameters of corresponding matrix, respectively.

In order to ensure the stability of the control system, the filter states are introduced into the original CM model, and q is replaced by q'. Consequently, an ECM involving notch filter is presented as follows:

$$\begin{aligned}
\dot{h} &= V \sin(\theta - \alpha), \\
\dot{V} &= \frac{1}{m}(T\cos\alpha - D) - g\sin(\theta - \alpha), \\
\dot{\alpha} &= \frac{1}{mV}(-T\sin\alpha - L) + q' + \frac{g}{V}\cos(\theta - \alpha), \\
\dot{\theta} &= q', \\
\dot{q}' &= c_{q1}\dot{x}_{q1} + c_{q2}\dot{x}_{q2} + \frac{d_q}{I_{yy}}(M + \tilde{\psi}_1\ddot{\eta}_1 + \tilde{\psi}_2\ddot{\eta}_2), \\
\ddot{\eta}_1 &= \frac{1}{k_1}\left(-2\zeta_1\omega_1\dot{\eta}_1 - \omega_1^2\eta_1 + N_1 - \tilde{\psi}_1\frac{M}{I_{yy}} - \frac{\tilde{\psi}_1\tilde{\psi}_2\ddot{\eta}_2}{I_{yy}}\right), \\
\ddot{\eta}_2 &= \frac{1}{k_2}\left(-2\zeta_2\omega_2\dot{\eta}_2 - \omega_2^2\eta_2 + N_2 - \tilde{\psi}_2\frac{M}{I_{yy}} - \frac{\tilde{\psi}_2\tilde{\psi}_1\ddot{\eta}_1}{I_{yy}}\right), \\
\dot{x}_{q1} &= a_{q1}x_{q1} + a_{q2}x_{q2} + b_{q1}q, \\
\dot{x}_{q2} &= a_{q3}x_{q1} + a_{q4}x_{q2} + b_{q2}q,
\end{aligned} \tag{40}$$

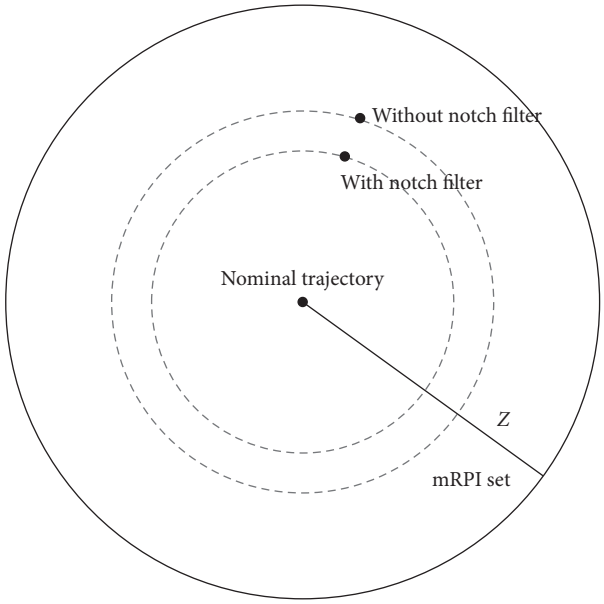

Figure 6: The state of system in the mRPI set at the same time.

4.2. Codesigned Polytopic LPV Modelling. Considering the weak coupling between flexible modes and rigid body, the ECM model is transformed into a control-oriented linearization model by using the same linearization method as above, where the notch filter is included.

In the flight envelope, the speed and altitude are also taken as the scheduling variables, and the corresponding system states and control inputs are defined as $x_s' = [h, V, \alpha, \theta, q\prime, \eta_1, \dot{\eta}_1, \eta_2, \dot{\eta}_2, x_{q1}, x_{q2}]^T, u_s' = [\Phi, \delta_e]^T$. The states at the equilibrium point can be obtained as

$$\begin{aligned}
x_r' &= \left[h_r, V_r, \alpha_r(h,V), \theta_r(h,V), q_r'(h,V), \eta_{1r}(h,V), \dot{\eta}_{1r}(h,V), \eta_{2r}(h,V), \dot{\eta}_{2r}(h,V), x_{q1r}(h,V), x_{q2r}(h,V)\right]^T, \\
u_r' &= \left[\Phi_r(h,V), \delta_{er}(h,V)\right]^T.
\end{aligned} \tag{41}$$

The corresponding LTI model can be built by Taylor expansion

$$\dot{x}'(t) = A'x'(t) + B'u'(t). \tag{42}$$

where

$$\begin{aligned}
x_s' &= \left[\Delta h, \Delta V, \Delta\alpha, \Delta\theta, \Delta q', \Delta\eta_1, \Delta\dot{\eta}_1, \Delta\eta_2, \Delta\dot{\eta}_2, \Delta x_{q1}, \Delta x_{q2}\right], \\
u' &= \left[\Delta\Phi, \Delta\delta_e\right], \\
A' &= \frac{\partial l(x_s', u_s')}{\partial x_s'}, B' = \frac{\partial l(x_s', u_s')}{\partial u_s'}.
\end{aligned} \tag{43}$$

Similarly, select different equilibrium points in the flight envelope for linearization and fitting to formulate the corresponding continuous LPV model:

$$\dot{x}'(t) = A'(p(t))x'(t) + B'(p(t))u'(t), \tag{44}$$

where $A'(p(t))$ and $B'(p(t))$ are matrices over scheduling variables.

Then, the discrete polytopic LPV model can be obtained by tensor product

$$x'(k+1) = A'(p(k))x'(k) + B'(p(k))u'(k). \tag{45}$$

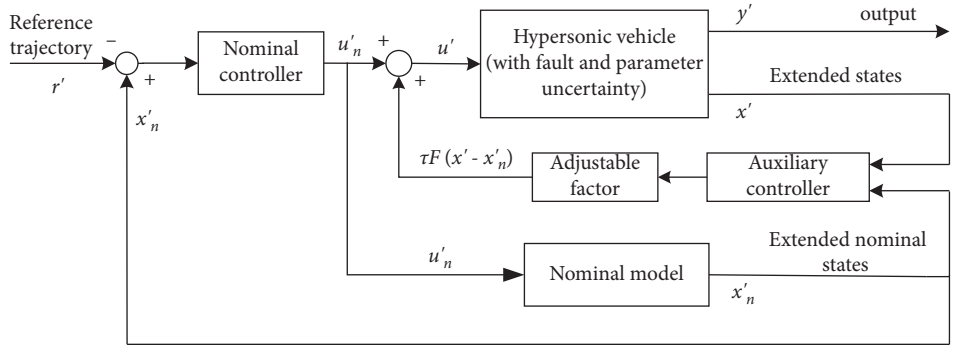

Figure 7: Adjustable control system scheme.

The corresponding nominal system has the following form

$$x_n'(k+1) = A'(p(k))x_n'(k) + B'(p(k))u_n'(k), \tag{46}$$

where, $x_n'(k), u_n'(k)$ are nominal system states and control inputs.

The comparison of Bode diagram is also given in Figure 8 to show the accuracy of the codesigned polytopic LPV model, in which the blue line represents the codesigned model and the red line for the ECM model. It can be seen that the new model can also conform to the frequency characteristics of the original model.

4.3. Adjustable Tube-MPC Controller Design. The baseline Tube-MPC controller is designed in the worst case of fault. However, in the actual flight, the worst case may not happen. In order to balance the control performance and robustness of system, an adjustable Tube-MPC control method is introduced [25].

Considering the case of incomplete actuator fault, the faulty model is formed as follows:

$$x'(k+1) = A'(p(k))x'(k) + B'(p(k))u'(k) + \Delta', \tag{47}$$

where $\Delta' \in W'$. W' denotes incomplete disturbance set, that is, $W' \subseteq W$. $u'(k)$ is the adjustable Tube-MPC control inputs, written as the following weighted formula:

$$u'(k) = \tau F'\left(x'(k) - x_n'(k)\right) + K'x_n'(k), \tag{48}$$

where τ is the adjustable factor. F' and K' are adjustable robust feedback gain and nominal control gain, respectively.

Firstly, the design method of F' is the same as the baseline controller by solving (19). It should be noted that the matrix in (19) should be expanded to the corresponding dimension.

Next, the invariant set is designed. In order to achieve better control performance, it is not necessary to choose the mRPI set Z for the extreme faults. The size of Z is positively correlated with the size of disturbance set W. Considering the nonworst case actuator fault, a smaller mRPI set Z' can be selected, where Z' is called incomplete disturbance mRPI (idmRPI) set. In this paper, an adjustable factor τ is used to regulate the size of mRPI set corresponding to incomplete fault. In general, τ should be a diagonal matrix representing the scaling degree of each dimension in Z. For simplicity, this paper considers that each dimension has the same scaling degree, so τ can be taken as a value from 0 to 1. Therefore, the relationship between Z and Z' can be expressed as $Z' = \tau Z$.

Finally, the adjustable nominal control law K' is designed. The following optimization problems are presented:

$$\min_{\gamma_n', Y', G', Q'} \gamma_n', \tag{49}$$

$$s.t \begin{bmatrix} 1 & x_n'(k)^T \\ x_n'(k) & Q' \end{bmatrix} \geq 0, \tag{50}$$

$$\begin{bmatrix} Q' & Q'^T A_i'^T + Y'^T B_i^T & Q'^T \psi'^{1/2T} & Y'^T \sigma'^{1/2T} \\ A_i'Q' + B_i'Y' & Q' & 0 & 0 \\ \psi'^{1/2T} Q' & 0 & \gamma_n' I' & 0 \\ \sigma'^{1/2T} Y' & 0 & 0 & \gamma_n' I' \end{bmatrix} > 0, \quad i \in \{1, 2, \ldots, R_l\}. \tag{51}$$

$$\begin{bmatrix} X' & Y' \\ Y'^T & Q' \end{bmatrix} \geq 0, X' = \begin{bmatrix} u_{n1}' & 0 \\ 0 & u_{n2}' \end{bmatrix}, u_{nj}' \leq u_{nj'\max}'^2, j = 1, 2, \tag{52}$$

where $Y' \in R^{2\times 11}$ is a matrix. $Q' \in R^{11\times 11}$ is a symmetric matrix. γ_n' is a positive scalar. $u_{nj,\max}'^2$ is the maximum of the jth adjustable nominal inputs satisfying the following constraint:

$$u_n' \in (U \Theta F' Z'). \tag{53}$$

Solving the above optimization problems, the adjustable nominal control law $K' = Y'Q'^{-1}$ can stabilize the system.

From (46), it can be seen that τ expands the constraint range of nominal control input. When τ is decreased, the nominal system constraint is relaxed such that the control performance becomes better and the robustness is worse. On the contrary, the nominal system constraints become strict such that the control performance decreases but the robustness of the system is improved. By adjusting τ, the stability of the closed-loop system can be further guaranteed.

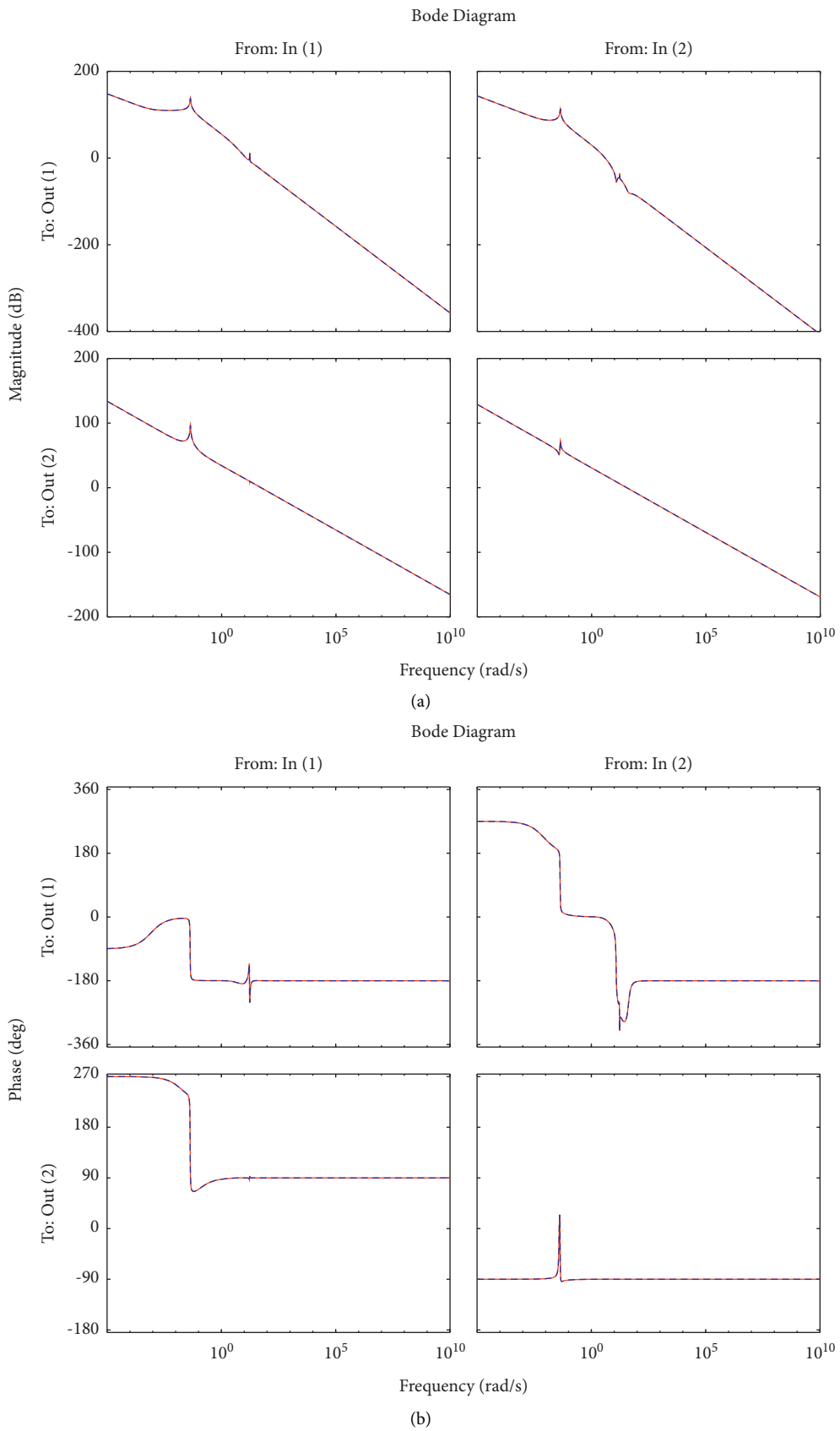

Figure 8: Bode diagram comparison of codesigned polytopic LPV model and ECM. (a) Amplitude frequency characteristics. (b) Phase frequency characteristics.

(1) Design parameters of notch filter
(2) Establish ECM model based on parameters of notch filter.
(3) Codesign the polytopic LPV model of flexible air-breathing hypersonic vehicle by Jacobi linearization and the tensor product based on ECM.
(4) Solve the robust auxiliary feedback control gain F' offline.
(5) Choose adjustable factor τ and compute the idmRPI set Z'.
(6) Calculate the nominal control gain K' offline.
(7) Apply the actual control law $u'_{total} = \tau F'(x' - x'_n) + K'x'_n + u'_r$ to the nonlinear model of flexible air-breathing hypersonic vehicle.

Algorithm 1: Steps of the proposed method.

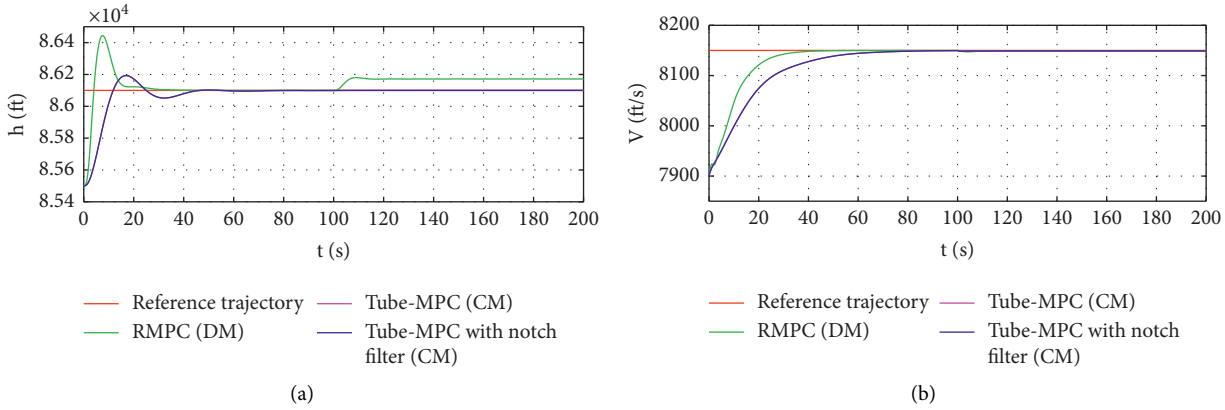

Figure 9: Trajectory in Case 1. (a) Altitude. (b) Velocity.

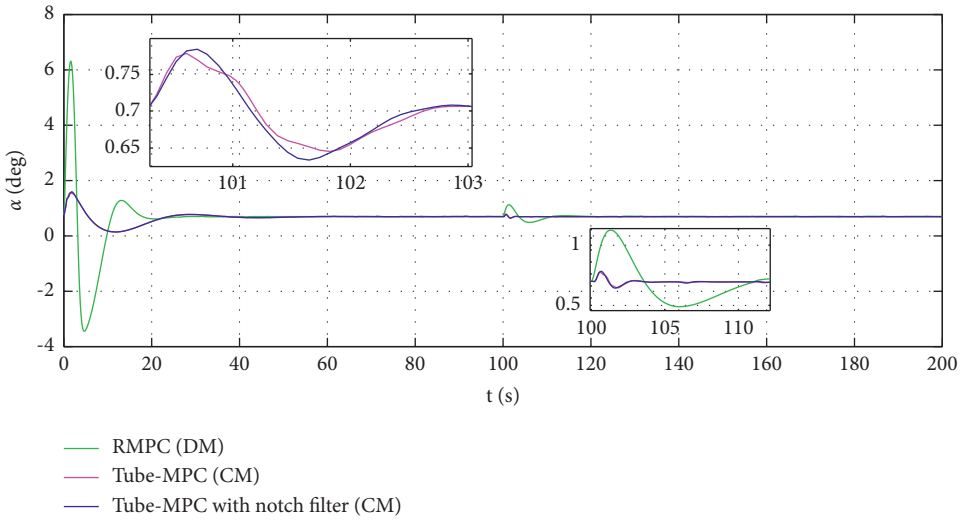

Figure 10: Continued.

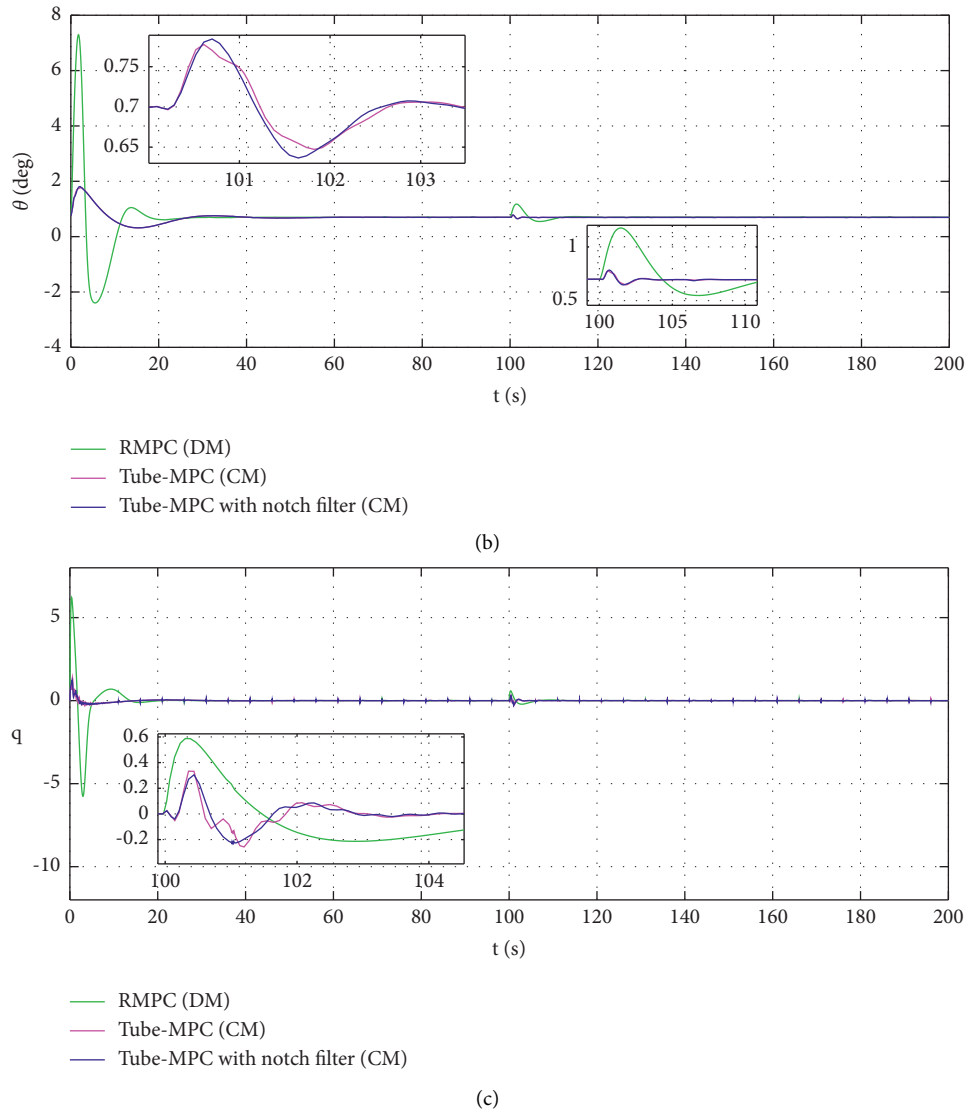

Figure 10: States in Case 1. (a) Attack angle. (b) Pitch angle. (c) Pitch rate.

4.4. The Real Control Law Is Written as

$$u'_{\text{total}} = \tau F'\left(x' - x'_n\right) + K'x'_n + u'_r \tag{54}$$

where u'_r is the control input at the equilibrium point.

The design steps of the adjustable design scheme are as follows.

5. Simulations

5.1. Simulation Conditions. Two cases are simulated to validate the effectiveness of the proposed method.

Case 1. In this case, the Tube-MPC controller via notch filter is verified. Select $\Gamma = [85000ft, 865000ft] \times [7700ft/s, 8300ft/s]$ as the flight envelope. And a polytopic LPV model with 20 vertices is built. The initial flight conditions are $h = 85500ft, V = 7900ft/s$. The commands are step signals: $600ft$ for height and $250ft/s$ for speed. The input constraints are $0 \le \Phi \le 1.5, -30^\circ \le \delta_e \le 30^\circ$. The maximum allowable error of longitudinal attitude angle is $\pm 0.5^\circ$. It is assumed that the loss of actuator effectiveness fault with 10% occurs at 100s, that is, $\rho_f = 0.9$. The uncertain parameters exist, given as $m < 10\%$, $I_{yy} < 10\%$, $S < 1\%$, $z_T < 1\%$, $\bar{c} < 1\%$, $c_e < 3\%$, $\beta_1 < 3\%$, $\beta_3 < 3\%$, $\beta_5 < 3\%$, $\beta_7 < 3\%$.

Case 2. In this case, the adjustable controller design scheme is verified. In the same flight envelope, the codesigned polytopic LPV model with 6 vertices is built. The command rises from $h = 85500ft$, $V = 7900ft/s$ to $h = 86100ft$, $V = 8150ft/s$ at a constant speed after 20 s. The adjustment factor $\tau = 0.8$. Parameter uncertainty and relevant parameters of fault are the same as Case 1.

5.2. Simulation Result and Analysis. To show the advantages of the controller designed in this paper, the traditional robust MPC (RMPC) is compared. It is worth noting that the

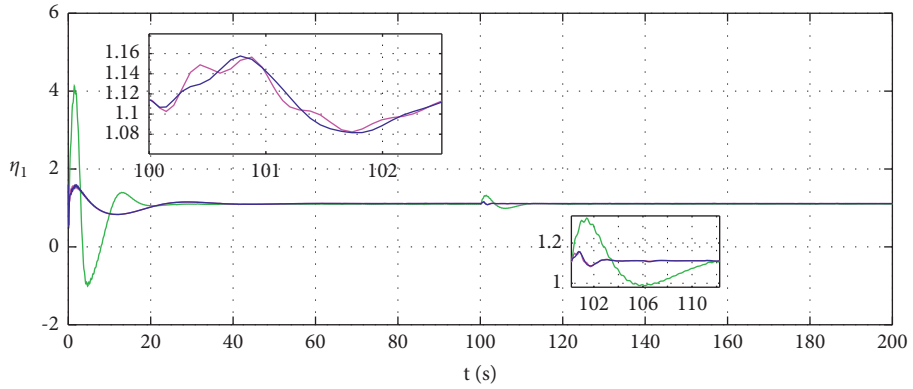

RMPC (DM)
Tube-MPC (CM)
Tube-MPC with notch filter (CM)

(a)

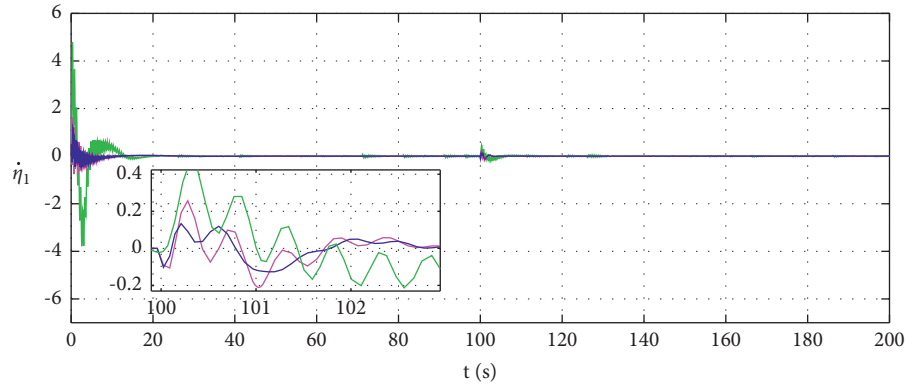

RMPC (DM)
Tube-MPC (CM)
Tube-MPC with notch filter (CM)

(b)

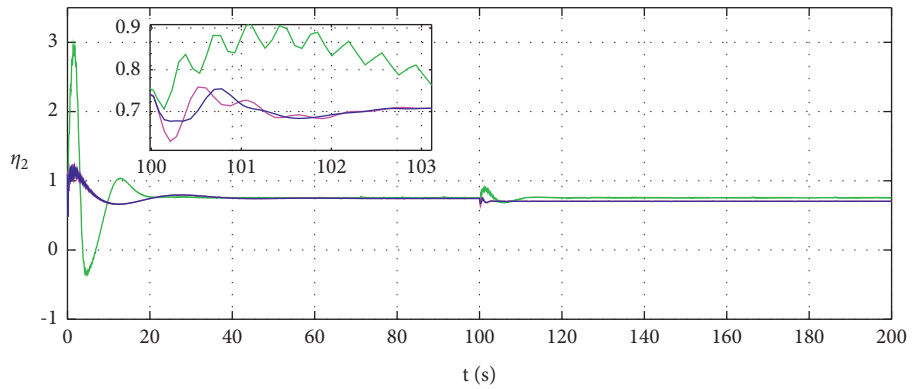

RMPC (DM)
Tube-MPC (CM)
Tube-MPC with notch filter (CM)

(c)

Figure 11: Continued.

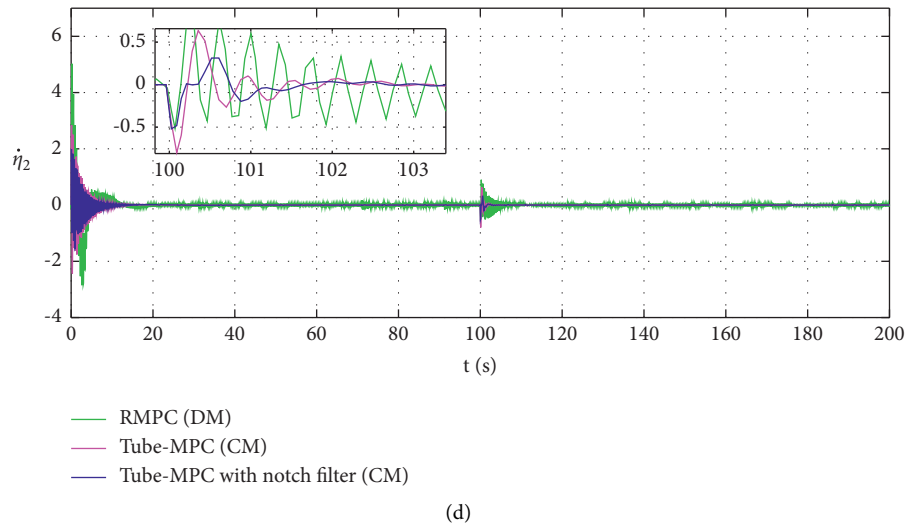

(d)

Figure 11: The generalized flexible coordinates of real system in Case 1. (a) The first-order generalized flexible coordinate. (b) Derivative of the first-order generalized flexible coordinate. (c) The second-order generalized flexible coordinate. (d) Derivative of the second-order generalized flexible coordinate.

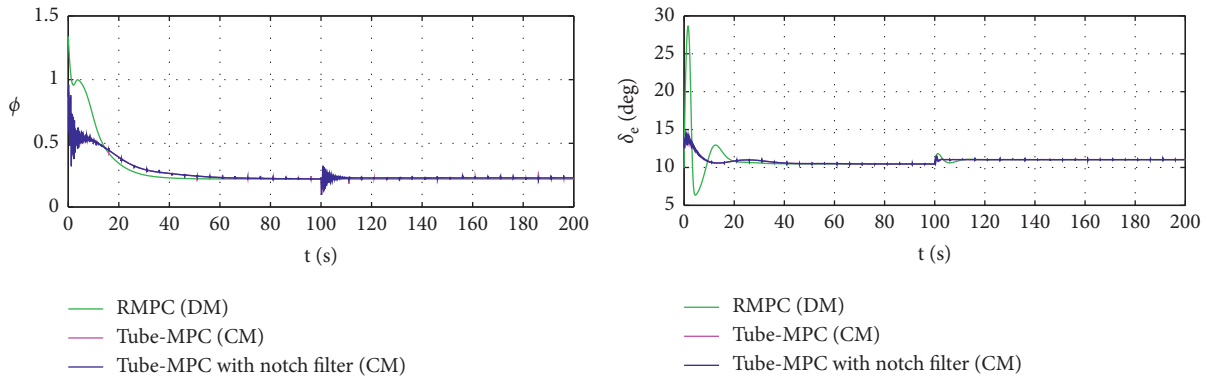

(a) (b)

Figure 12: Control inputs in Case 1. (a) Fuel-to-air ratio. (b) Elevator deflection.

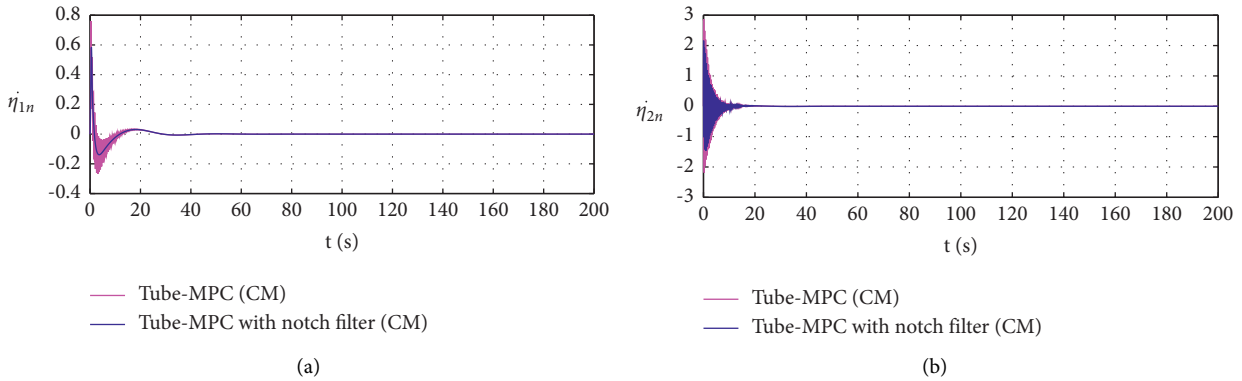

(a) (b)

Figure 13: Derivative of the generalized flexible coordinates of nominal system in the case of notch filter for the second-order flexible mode. (a) Derivative of the first-order generalized flexible coordinate. (b) Derivative of the second-order generalized flexible coordinate.

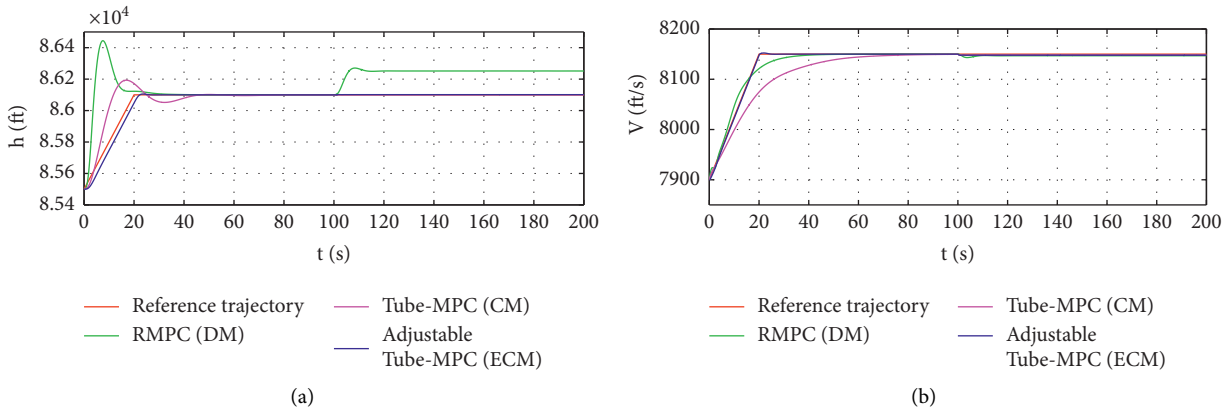

Figure 14: Trajectory in case 2. (a) altitude. (b) Velocity.

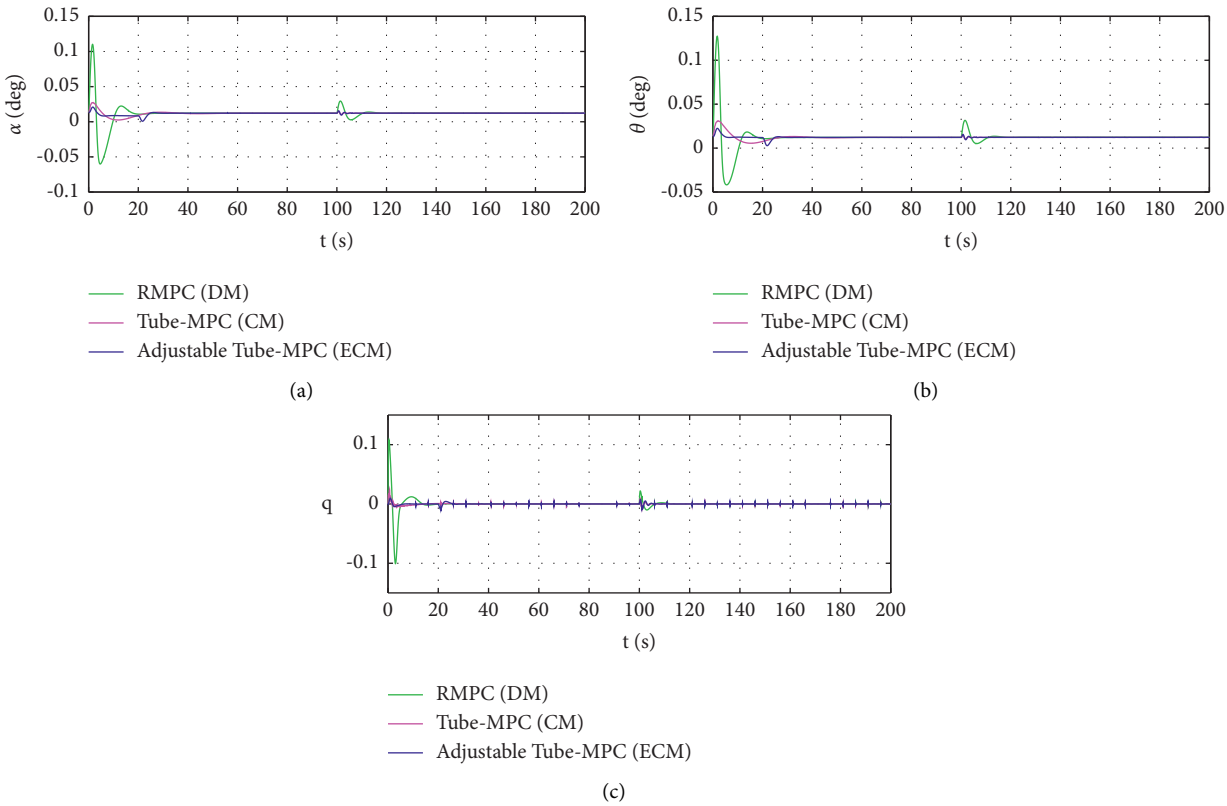

Figure 15: States in Case 2. (a) Attack angle. (b) Pitch angle. (c) Pitch rate.

traditional RMPC cannot achieve satisfactory result in the presence of flexibility. So the traditional RMPC is just used to control the DM (4) without flexibility.

Figure 9 shows the height and velocity trajectory tracking results in the presence of parameter uncertainty and actuator fault of loss of effectiveness. After fault happens, the flexible hypersonic vehicle can still track the reference trajectory stably using Tube-MPC. However, the accurate altitude tracking is not achieved by the traditional RMPC. Figure 10 shows attack angle, pitch angle, and pitch rate vibrate when fault occurs but soon stabilize at equilibrium. Compared with the traditional RMPC, the vibration is smaller. Compared with Tube-MPC without notch filter, the state change of Tube-MPC with notch filter is gentler and smoother after fault occurs. Figure 11 shows the curves of the generalized flexible coordinates and their derivatives. They vibrate after fault occurs, but soon return to stability. Similarly, using the traditional RMPC control, they vibrate a lot more. The jitter of the system under Tube-MPC with notch filter is gentler and smoother. Figure 12 shows the curves of the control inputs. It can be seen that control inputs satisfy the input constraints in presence of fault.

The notch filter in the above simulation is designed for the first-order elastic mode. To show its power further, the

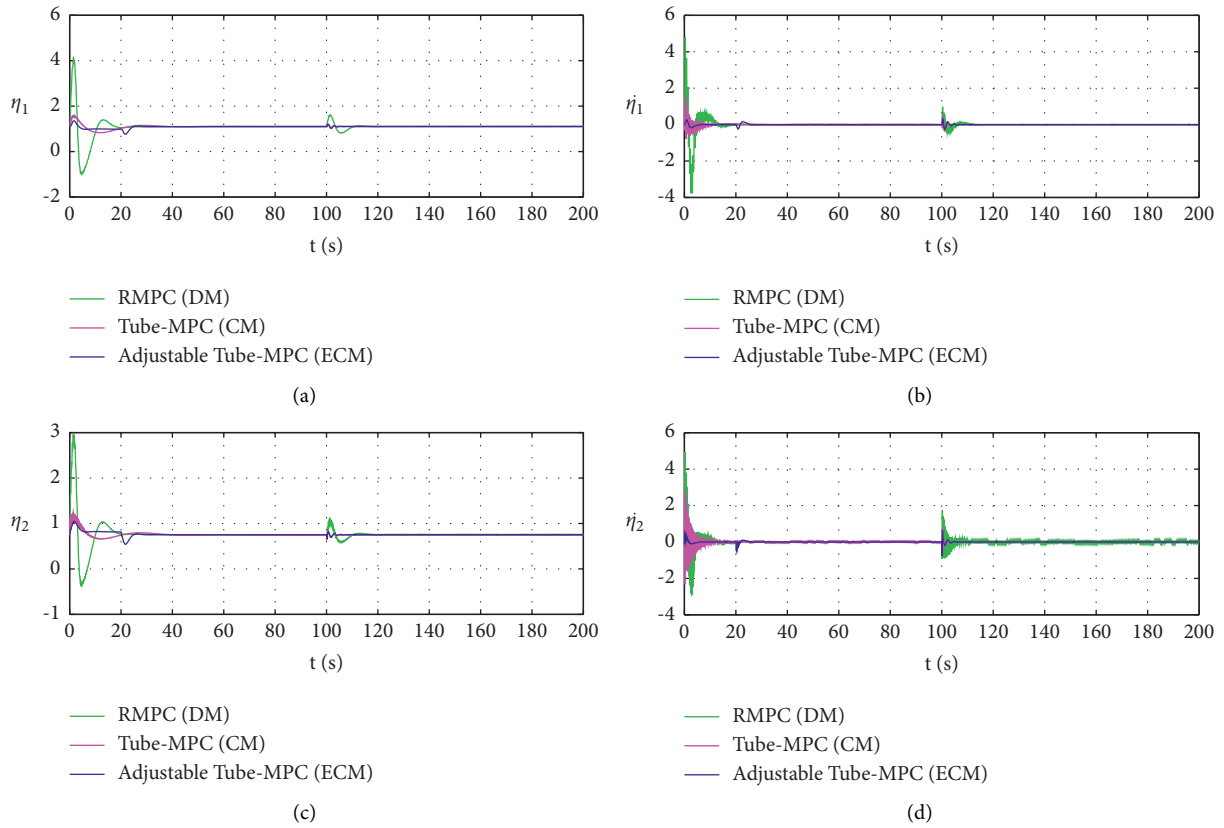

Figure 16: The generalized flexible coordinates of real system in Case 2. (a) The first-order generalized flexible coordinate. (b) Derivative of the first-order generalized flexible coordinate. (c) The second-order generalized flexible coordinate. (d) Derivative of the second-order generalized flexible coordinate.

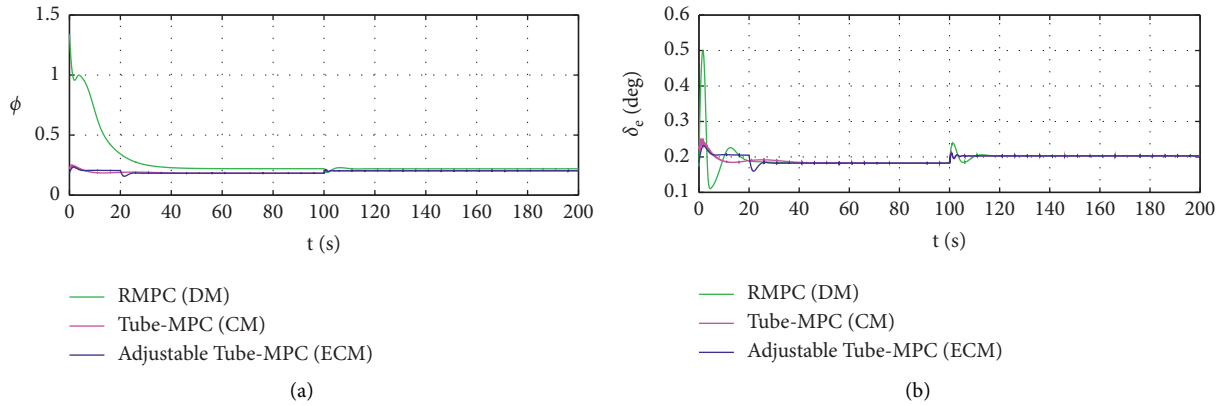

Figure 17: Control inputs in Case 2. (a) Fuel-to-air ratio. (b) Elevator deflection.

second-order flexible mode is addressed separately by notch filter, shown in Figure 13. It can be known that the notch filter has a slight inhibition on the derivative of the first-order flexible mode, and a significant impact on the derivative of the second-order flexible mode.

Simulation results show that the Tube-MPC with notch filter can realize accurate and stable trajectory tracking in presence of uncertain parameters and actuator loss of effectiveness fault. The dynamic error of the longitudinal attitude angles is within $\pm 0.5^{\circ}$. By introducing notch filter, the flexible modes can be rejected.

As can be seen from Figures 14 and 15, the adjustable control scheme not only ensures the stability of the aircraft, but also improves the rapidity of speed response. In Figure 16, the adjustable controller can get rid of the influence of elastic characteristics. As can be seen from Figure 17, in case of failure, the control inputs of the adjustable method can still be maintained within a reasonable range.

6. Conclusion

In this paper, Tube-MPC via notch filter trajectory tracking controller are designed for flexible air-breathing hypersonic vehicle with parameter uncertainty and actuator fault. Firstly, the polytopic LPV model is established by Jacobian linearization and tensor product. The parameter uncertainty and actuator fault are uniformly transformed into the lumped term. The Tube-MPC controller is designed, where the actual trajectory is limited to the mRPI set and is able to approximate the nominal trajectory. The notch filter is introduced to eliminate flexibility. To ensure the stability of the closed-loop system, the adjustable control scheme is proposed. The filter and the original nonlinear model are combined to formulate the ECM model. Based on the codesigned polytopic LPV model, the adjustable Tube-MPC controller is designed to balance control performance and robustness. The simulation results show the effectiveness of the two controllers. Online identification of flexibility of hypersonic vehicle will be considered in future research.

Data Availability

The data of structural and aerodynamic parameters of flexible air-breathing hypersonic vehicle used to support the findings of this study are included in "Control-Oriented Modeling of an Air-Breathing Hypersonic Vehicle" (DOI: 10.2514/1.27830), which are cited within the text as reference [8]. The simulation conditions' data used to support the findings of this study are included within the article.

Conflicts of Interest

The authors declare that there are no conflicts of interest regarding the publication of this article.

Acknowledgments

This work was supported by Aeronautical Science Foundation of China (20180748002) and Tianjin University Innovation Foundation (2022XSU-0003).

References

[1] H. An, Q. Q. Wu, C. H. Wang, and Cao, "Scramjet operation guaranteed longitudinal control of air-breathing hypersonic vehicles," *IEEE/ASME Transactions on mechatronics*, vol. 25, no. 6, pp. 2587–2598, 2020.

[2] P. Gruhn and A. Gülhan, "Aerodynamic measurements of an air-breathing hypersonic vehicle at mach 3.5 to 8," *AIAA Journal*, vol. 56, no. 11, pp. 4282–4296, 2018.

[3] M. A. Bolender and D. B. Doman, "Nonlinear longitudinal dynamical model of an air-breathing hypersonic vehicle," *Journal of Spacecraft and Rockets*, vol. 44, no. 2, pp. 374–387, 2007.

[4] M. R. Waszak and D. K. Schmidt, "Flight dynamics of aeroelastic vehicles," *Journal of Aircraft*, vol. 25, no. 6, pp. 563–571, 2012.

[5] P. R. Sudalagunta, C. Sultan, R. K. Kapania et al., "Aeroelastic control-oriented modeling of an airbreathing hypersonic vehicle," *Journal of Guidance, Control, and Dynamics*, vol. 44, no. 2, pp. 1136–1149, 2018.

[6] L. Fiorentini, "Nonlinear adaptive controller design for air-breathing hypersonic vehicles," *Columbus: Ohio State University*, 2010.

[7] D. O. Sigthorsson and A. Serrani, "Development of linear parameter-varying models of hypersonic air-breathing vehicles," *Proceedings of the AIAA Guidance, Navigation, and Control Conference*, pp. 1–21, Chicago, August 2009.

[8] J. T. Parker, M. A. Serrani, D. B. Yurkovich, Bolender, and Doman, "Control-oriented modeling of an air-breathing hypersonic vehicle," *Journal of Guidance, Control, and Dynamics*, vol. 30, no. 3, pp. 856–869, 2007.

[9] L. Cao, S. Tang, and D. Zhang, "Flight control for air-breathing hypersonic vehicles using linear quadratic regulator design based on stochastic robustness analysis," *Frontiers of Information Technology & Electronic Engineering*, vol. 18, no. 7, pp. 882–897, 2017.

[10] H. An and Q. Q. Wu, "Anti-windup disturbance suppression control of feedback linearizable systems with application to hypersonic flight vehicles," *Proceedings of the Institution of Mechanical Engineers - Part G: Journal of Aerospace Engineering*, vol. 233, no. 11, pp. 3952–3967, 2019.

[11] H. B. Sun, S. H. Li, J. Yang, and Guo, "Non-linear disturbance observer-based back-stepping control for airbreathing hypersonic vehicles with mismatched disturbances," *IET Control Theory & Applications*, vol. 8, no. 17, pp. 1852–1865, 2014.

[12] Z. G. Guo, J. G. Guo, J. Chang, and Zhou, "Coupling effect-triggered control strategy for hypersonic flight vehicles with finite-time convergence," *Nonlinear Dynamics*, vol. 95, no. 2, pp. 1009–1025, 2019.

[13] B. Xu, X. Wang, and Z. K. Shi, "Robust adaptive neural control of nonminimum phase hypersonic vehicle model," *IEEE Transactions on Systems, Man, and Cybernetics: Systems*, vol. 51, no. 2, pp. 1107–1115, 2021.

[14] X. L. Tao, J. Q. Yi, Z. Q. Pu, and Xiong, "Robust adaptive tracking control for hypersonic vehicle based on interval type-2 fuzzy logic system and small-gain approach," *IEEE Transactions on Cybernetics*, vol. 51, no. 5, pp. 2504–2517, 2021.

[15] H. W. Zhao and R. Li, "Typical adaptive neural control for hypersonic vehicle based on higher-order filters," *Journal of Systems Engineering and Electronics*, vol. 31, pp. 1031–1040, 2020.

[16] Y. Q. Huang, C. Y. Sun, C. S. Qian, Zhang, and Wang, "Polytopic LPV modeling and gain-scheduled switching control for a flexible air-breathing hypersonic vehicle," *Journal of Systems Engineering and Electronics*, vol. 24, no. 1, pp. 118–127, 2013.

[17] L. X. Zhang, L. Nie, B. Cai, Yuan, and Wang, "Switched linear parameter-varying modeling and tracking control for flexible hypersonic vehicle," *Aerospace Science and Technology*, vol. 95, p. 105445, 2019.

[18] L. G. Wu, X. B. Yang, and F. B. Li, "Nonfragile output tracking control of hypersonic air-breathing vehicles with an LPV model," *IEEE*, vol. 18, no. 4, pp. 1280–1288, 2013.

[19] B. Xu, D. W. Wang, Y. M. Zhang, and Shi, "DOB-based neural control of flexible hypersonic flight vehicle considering wind effects," *IEEE Transactions on Industrial Electronics*, vol. 64, no. 11, pp. 8676–8685, 2017.

[20] J. L. Sun, J. Q. Yi, Z. Q. Pu, and Tan, "Fixed-time sliding mode disturbance observer-based nonsmooth backstepping control for hypersonic vehicles," *IEEE Transactions on Systems, Man, and Cybernetics: Systems*, vol. 50, no. 11, pp. 4377–4386, 2020.

[21] K. Y. Hu, F. Y. Chen, and Z. Cheng, "Fuzzy adaptive hybrid compensation for compound faults of hypersonic flight vehicle," *International Journal of Control, Automation and Systems*, vol. 19, no. 6, pp. 2269–2283, 2021.

[22] D. Zhao, B. Jiang, H. Yang, and Tao, "Fault-tolerant control of flexible air-breathing hypersonic vehicles in linear ODE-beam systems," *International Journal of Control*, vol. 93, no. 4, pp. 820–831, 2020.

[23] H. An, J. X. Liu, C. H. Wang, and Wu, "Approximate backstepping fault-tolerant control of the flexible air-breathing hypersonic vehicle," *IEEE*, vol. 21, no. 3, pp. 1680–1691, 2016.

[24] X. L. Shao, Y. Shi, and W. D. Zhang, "Fault-tolerant quantized control for flexible air-breathing hypersonic vehicles with appointed-time tracking performances," *IEEE Transactions on Aerospace and Electronic Systems*, vol. 57, no. 2, pp. 1261–1273, 2021.

[25] C. F. Hu, X. F. Wei, and Y. L. Ren, "Passive fault-tolerant control based on weighted LPV tube-MPC for air-breathing hypersonic vehicles," *International Journal of Control, Automation and Systems*, vol. 17, no. 8, pp. 1957–1970, 2019.

[26] Z. F. Gao, J. X. Lin, and T. Cao, "Robust fault tolerant tracking control design for a linearized hypersonic vehicle with sensor fault," *International Journal of Control, Automation and Systems*, vol. 13, no. 3, pp. 672–679, 2015.

[27] J. C. Hu and B. C. Ding, "A periodic approach to dynamic output feedback MPC for quasi-LPV model," *IEEE Transactions on Automatic Control*, pp. 1–8, 2020.

[28] B. C. Ding and H. G. Pan, "Output feedback robust MPC for LPV system with polytopic model parametric uncertainty and bounded disturbance," *International Journal of Control*, vol. 89, no. 8, pp. 1554–1571, 2016.

[29] L. Cui, L. Chen, and D. P. Duan, "Gain-scheduling model predictive control for unmanned airship with LPV system description," *Journal of Systems Engineering and Electronics*, vol. 26, no. 5, pp. 1043–1051, 2015.

[30] D. Gángó, T. Péni, and R. Tóth, "Learning based approximate model predictive control for nonlinear system," *IFAC-PapersOnLine*, vol. 52, no. 28, pp. 152–157, 2019.

[31] J. C. Hu and B. C. Ding, "One-step ahead robust MPC for LPV model with bounded disturbance," *European Journal of Control*, vol. 52, pp. 59–66, 2020.

[32] P. Bumroongsri, "Tube-based robust MPC for linear time-varying systems with bounded disturbances," *International Journal of Control, Automation and Systems*, vol. 13, no. 3, pp. 620–625, 2015.

[33] P. Baranyi, "TP model transformation as a way to LMI-based controller design," *IEEE Transactions on Industrial Electronics*, vol. 51, no. 2, pp. 387–400, 2004.

[34] Y. Su, K. K. Tan, and T. H. Lee, "Tube based quasi-min-max output feedback MPC for LPV Systems1," *IFAC Proceedings Volumes*, vol. 45, no. 15, pp. 186–191, Singapore, 2012.

[35] S. V. Rakovic, E. C. Kerrigan, K. I. Kouramas, and Mayne, "Invariant approximations of the minimal robust positively invariant set," *IEEE Transactions on Automatic Control*, vol. 50, no. 3, pp. 406–410, 2005.

[36] F. Tahir, "Efficient computation of robust positively invariant sets with linear state-feedback gain as a variable of optimization," *Proceedings of the 7th International Conference on Electrical Engineering, Computing Science and Automatic Control*, pp. 199–204, Tuxtla Gutierrez, Mexico, September 2010.

[37] M. V. Kothare, V. Balakrishnan, and M. Morari, "Robust constrained model predictive control using linear matrix inequalities," *Automatica*, vol. 32, no. 10, pp. 1361–1379, 1996.

[38] Z. G. Meng and J. Yan, "Adaptive modal suppression for hypersonic aeroelastic vehicle," *Journal of Astronautics*, vol. 32, no. 10, pp. 2164–2168, 2011.

[39] J. Levin, P. A. Ioannou, and M. D. Mirmirani, "Adaptive mode suppression scheme for an aeroelastic airbreathing hypersonic cruise vehicle," *Proceedings of the AIAA Guidance, Navigation and Control Conference and Exhibit*, pp. 1–12, Honolulu, HI, USA, August 2008.

[40] Z. Q. Pu, R. Y. Yuan, X. M. Tan, and Yi, "Active robust control of uncertainty and flexibility suppression for air-breathing hypersonic vehicles," *Aerospace Science and Technology*, vol. 42, pp. 429–441, 2015.